

CHARACTERIZATION OF POLYDISPERSE
COLLOIDS BY FIELD-FLOW FRACTIONATION
(FFF): DETERMINATION OF SIZE AND
COMPOSITION OF SOIL COLLOIDS

ARTHUR LAKES LIBRARY
COLORADO SCHOOL OF MINES
GOLDEN, CO 80401

by

Daniel J. Dawson

ProQuest Number: 10794614

All rights reserved

INFORMATION TO ALL USERS

The quality of this reproduction is dependent upon the quality of the copy submitted.

In the unlikely event that the author did not send a complete manuscript and there are missing pages, these will be noted. Also, if material had to be removed, a note will indicate the deletion.



ProQuest 10794614

Published by ProQuest LLC (2018). Copyright of the Dissertation is held by the Author.

All rights reserved.

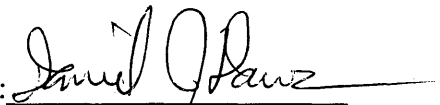
This work is protected against unauthorized copying under Title 17, United States Code
Microform Edition © ProQuest LLC.

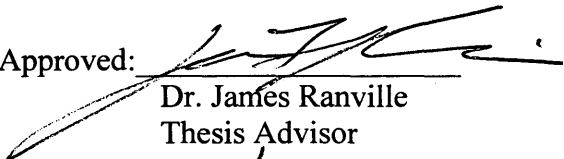
ProQuest LLC.
789 East Eisenhower Parkway
P.O. Box 1346
Ann Arbor, MI 48106 – 1346

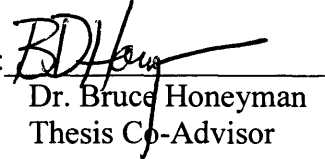
A thesis submitted to the Faculty and Board of Trustees of the Colorado School of Mines in partial fulfillment of the requirements for the degree of Master of Science (Environmental Science and Engineering).

Golden, Colorado

Date 1/2/02

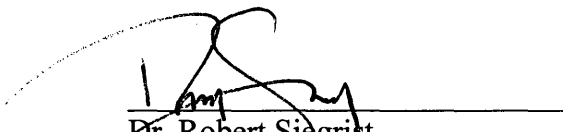
Signed: 
Daniel J. Dawson

Approved: 
Dr. James Ranville
Thesis Advisor

Approved: 
Dr. Bruce Honeyman
Thesis Co-Advisor

Golden, Colorado

Date: JAN 02, 2002


Dr. Robert Siegrist
Professor and Head,
Department of Environmental
Science and Engineering

ABSTRACT

Mobile soil colloids are thought to play a major role in the transportation of contaminants through porous subsurface media. The basic principles of flow through porous media establish that diffusion and sedimentation (filtration) of colloidal material may be responsible for removal of smaller and larger sized particles respectively. Using this theory, it is hypothesized that particles of a certain size will have the highest potential to move through the media without being affected by diffusion or sedimentation. This increases the probability of transport of non-aqueous contaminants if they adsorb onto the surface of the colloids.

Presently, the most common separation of heterogeneous sized colloidal material is through high-speed centrifugation. Centrifugation can be fairly accurate in the separation of calculated size ranges of spherical particles. When the particle sizes are very fine, however, centrifugation has a disadvantage of long settling times. In addition, proper size separation may require multiple runs and there is no size analysis available.

Presently, several methods exist to conduct particle size analysis. Most commonly utilized techniques include photon correlation spectroscopy (PCS), scanning electron microscopy (SEM), single particle optical sensing (SPOS), and field-flow fractionation (FFF). FFF is a relatively new technique capable of separation of particles based upon size, which are capable of accurately separating macromolecules, colloids, and particulate materials with sizes from 10^{-3} to 10^2 μm . These particles can include materials such as polystyrene beads, viruses, bacteria, and heterogeneous soil colloids. The high resolution of the FFF, with its short runs, make FFF a valuable tool towards characterization of soils.

A valuable characteristic of FFF is the ability to couple elemental analysis instruments such as inductively coupled plasma (ICP) and atomic absorption

spectrometry (AAS) with the size distribution from the FFF, which can be beneficial in determining a potential change in mineralogy and surface coatings of natural soil colloids. By determining the surface charge of the colloids, in addition to the mineralogy and the presence of any surface coatings, it is possible to determine if there is a potential for contaminant adsorption. This can then imply the transportation of these colloids and the contaminants through porous subsurface media.

TABLE OF CONTENTS

ABSTRACT.....	iii
LIST OF FIGURES	vii
LIST OF TABLES.....	x
ACKNOWLEDGMENTS	xi
 Chapter 1 – INTRODUCTION.....	 1
1.1 Colloidal Particles	1
1.2 Colloid Transport Potential	4
1.3 Purpose of Project	5
1.4 Structure of Thesis.....	9
 Chapter 2 – PARTICLE SIZING METHODS	
2.1 Introduction	10
2.2 Theory and Basis of Operation for Size Analysis Methods	12
2.2.1 Stokes Law of Settling.....	12
2.2.2 Brownian Motion	14
2.3 Particle Sizing Methods.....	14
2.3.1 Single Particle Optical Sensor	14
2.3.2 Photon Correlation Spectroscopy	16
2.3.3 Scanning Electron Microscopy	17
2.3.4 Field Flow Fractionation.....	18
2.3.4.1 Normal Mode Elution	20
2.3.4.1.1 Flow FFF Theory	22
2.3.4.1.2 Sedimentation FFF Theory	24
2.3.4.2 Steric Mode Elution	25
2.3.4.3 Representation of the Data.....	26
2.4 Experimental Design	26
2.4.1 Soil Preparation.....	28

2.4.2	Prefractionation by Centrifugation	29
2.4.3	FFF Setup.....	30
2.4.3.1	FIFFF Design	30
2.4.3.2	SdFFF Design	31
2.5	Results and Discussion.....	32
2.5.1	Centrifugation	32
2.5.2	SPOS.....	34
2.5.3	PCS	35
2.5.4	SEM	38
2.5.5	FFF	42
2.5.5.1	Normal Mode Elution	42
2.5.5.2	Steric Mode Elution	50
2.6	Conclusion.....	52
Chapter 3 – CHEMICAL ANALYSIS VERSUS SIZE		58
3.1	Introduction	58
3.2	Analytical Chemistry Techniques Utilized to Determine Elemental Composition	59
3.2.1	Inductively Coupled Plasma-Mass Spectrometry	60
3.2.2	Graphite Furnace Atomic Absorption Spectrometer	61
3.3	Results and Discussion.....	62
3.3.1	Offline Coupling of FIFFF to GFAAS.....	62
3.3.2	Online Coupling of SdFFF to ICP-MS	65
3.3.2.1	Analysis of the <0.2 Micron Rocky Flats Soil Fraction	65
3.3.2.2	Analysis of the 0.2-0.8 Micron Rocky Flats Soil Fraction	73
3.4	Conclusion.....	80
Chapter 4 – SUMMARY AND CONCLUSIONS.....		86
4.1	Summary of Results	86
4.2	Recommendations for Future Research	87
REFERENCES CITED.....		88

LIST OF FIGURES

Figure 1.1:	Particle sizing of colloidal and particulates for natural waters (Ranville and Schmiermund, 1998).	2
Figure 1.2:	Particle collection efficiencies of colloidal particles in a porous media. (Yao, Habibian and O'Melia, 1971).....	6
Figure 1.3:	Representation of colloidal transport mechanisms in groundwater through a porous media	7
Figure 2.1:	Representation of particle separations through an FFF channel using normal mode	20
Figure 2.2a:	Normal mode elution FIFFF run of five polystyrene beads displaying the fractogram with UV response plotted against time	27
Figure 2.2b:	Normal mode elution FIFFF run of five polystyrene beads displaying the converted size distribution of relative amount versus diameter	27
Figure 2.3:	Experimental design setup of an FIFFF channel (FFFractionation website).....	31
Figure 2.4:	Experimental design of the SdFFF channel depicting potential coupling of chemical analysis instruments such as ICP-MS and GFAAS	33
Figure 2.5:	SPOS analysis of the 0.8-2.0 μm fraction of Rocky Flats soils.....	36
Figure 2.6:	SPOS analysis of the 2.0-10 μm fraction of Rocky Flats soils.....	37
Figure 2.7:	SEM experimental results of the <0.2 micron Rocky Flats soil fraction	39
Figure 2.8:	SEM experimental results of the 0.2-0.8 micron Rocky Flats soil fraction	40
Figure 2.9:	SEM experimental results of the 0.8-2.0 micron Rocky Flats soil fraction	41

Figure 2.10:	SEM experimental results of the 2.0-10 micron Rocky Flats soil fraction	43
Figure 2.11a:	Results of the <0.2 μm soil fraction using the SdFFF and FIFFF under normal mode conditions.....	45
Figure 2.11b:	Converted fractogram into diameter versus relative amount of the <0.2 μm soil fraction	45
Figure 2.12:	Fractogram illustrating the <0.2 μm soil fraction elemental aluminum mass versus UV response of the SdFFF	47
Figure 2.13a:	Results of the 0.2-0.8 μm soil fraction using the SdFFF and FIFFF under normal mode conditions.....	48
Figure 2.13b:	Converted fractogram into diameter versus relative amount of the 0.2-0.8 μm soil fraction	48
Figure 2.14:	Fractogram illustrating the 0.2-0.8 μm soil fraction elemental aluminum mass versus UV response of the SdFFF	49
Figure 2.15a:	Results of the 0.8-2.0 μm soil fraction using the FIFFF under steric mode conditions	51
Figure 2.15b:	Converted fractogram into diameter versus relative amount of the 0.8-2.0 μm soil fraction	51
Figure 2.16a:	Results of the 2.0-10 μm soil fraction using the FIFFF under steric mode conditions	53
Figure 2.16b:	Converted fractogram into diameter versus relative amount of the 2.0-10 μm soil fraction	53
Figure 2.17:	Comparison of the results of the SEM for the soil fractions	56
Figure 2.18:	Comparison of the results of the FIFFF for the soil fractions.....	57
Figure 3.1a:	Results of offline coupling of GFAAS with FIFFF yielding Fe concentration, UV response, and the Fe/Al ratio.....	64
Figure 3.1b:	GFAAS and FIFFF offline coupling showing UV response versus Fe concentration.....	64
Figure 3.2a:	Comparative fractogram of mass Si and UV response for the SdFFF coupled with ICP-MS of the <0.2 μm soil fraction	66
Figure 3.2b:	Converted fractogram into relative amount versus diameter for the Si and UV of the <0.2 μm soil fraction	66

Figure 3.3a:	Comparative fractogram of mass Al, Fe, and UV response for the SdFFF coupled with ICP-MS of the <0.2 μm soil fraction.....	68
Figure 3.3b:	Representative ratios of the Al/Si and Fe/Si for the <0.2 μm soil fraction versus diameter.....	68
Figure 3.3c:	Converted fractogram into relative amount versus diameter for the Al, Fe, and UV of the <0.2 μm soil fraction	69
Figure 3.4:	Representative ratios of the Mg/Si and K/Si for the <0.2 μm soil fraction versus diameter.....	71
Figure 3.5a:	Comparative fractogram of mass Mn, U, and UV response for the SdFFF coupled with ICP-MS of the <0.2 μm soil fraction.....	72
Figure 3.5b:	Representative ratios of the Mn/Si and U/Si for the <0.2 μm soil fraction versus diameter.....	72
Figure 3.5c:	Converted fractogram into relative amount versus diameter for the Mn, U, and UV of the <0.2 μm soil fraction.....	74
Figure 3.6a:	Comparative fractogram of mass Si and UV response for the SdFFF coupled with ICP-MS of the 0.2-0.8 μm soil fraction	75
Figure 3.6b:	Converted fractogram into relative amount versus diameter for the Si and UV of the 0.2-0.8 μm soil fraction.....	75
Figure 3.7a:	Comparative fractogram of mass Al, Fe, and UV response for the SdFFF coupled with ICP-MS of the 0.2-0.8 μm soil fraction	77
Figure 3.7b:	Representative ratios of the Al/Si and Fe/Si for the 0.2-0.8 μm soil fraction versus diameter	77
Figure 3.7c:	Representative ratios of the Mg/Si and K/Si for the 0.2-0.8 μm soil fraction versus diameter	78
Figure 3.7d:	Converted fractogram into relative amount versus diameter for the Al, Fe, and UV of the 0.2-0.8 μm soil fraction	79
Figure 3.8a:	Comparative fractogram of mass Mn, U, and UV response for the SdFFF coupled with ICP-MS of the 0.2-0.8 μm soil fraction	81
Figure 3.8b:	Representative ratios of the Mn/Si and U/Si for the <0.2 μm soil fraction versus diameter.....	81
Figure 3.8c:	Converted fractogram into relative amount versus diameter for the Mn, U, and UV of the <0.2 μm soil fraction.....	82

LIST OF TABLES

Table 2.1:	Bulk size distribution of Rocky Flats soils	34
Table 2.2:	PCS mean data size of Rocky Flats soil fractions.....	35
Table 2.3:	Conditions used for particle separations of Rocky Flat soil fractions.....	44
Table 2.4:	Mean size distribution of the Rocky Flats colloids using the various particle-sizing methods	54
Table 3.1:	SdFFF conditions used for size analysis of the soil fractions.....	63
Table 3.2:	Percentage of elemental mass in Rocky Flats soils obtained by integration of the SdFFF-ICP-MS results	83
Table 3.3a:	Comparison of elemental ratios of bulk fraction and FFF run elution from channel using Al to compare	84
Table 3.3b:	Comparison of elemental ratios of bulk fraction and FFF run elution from channel using Si to compare the elements	84

ACKNOWLEDGMENTS

While the majority of the hands on work has been conducted by myself, this project could not have been completed without the compilation of help by a large number of people with brainstorming, emotional support, and financial support.

First, I must express my sincere appreciation to my advisors, Drs. James Ranville and Bruce Honeyman, who have given me this great opportunity to work with them and help broaden my intellectual ability. They have been most responsible for the work that has been completed, seeing the holes in the research that needed to be filled in, and interpreting the results that I generated. Special thanks must be given to Jim for all the hard work in molding my writing into something decipherable in such a short period of time.

I must also extend special thanks to my committee members, Drs. Ron Cohen and John Seaman for all the interest that they have shown in my work. Dr. John Seaman, an off-campus committee member who works for the University of Georgia at the Savannah River Ecology Laboratory, is largely responsible for my funding. Funding also came graciously from the EPA and NIH.

In addition, I owe sincere thanks to Dr. Richard Murphy, Dr. Cetin Kantar, Ruth Tinnacher, Lee Landkamer, Dr. Brian Jackson, Anthony Bednar, Joshua Pearson, Peter Hicks, and LaDonna Choate for all the help that they gave along the way.

I have also been graced with having an understanding family and a large number of wonderful friends who have helped me enormously in emotional support and encouragement along the way.

CHAPTER 1

INTRODUCTION

1.1 Colloidal Particles

Environmental soil colloids are particles of heterogeneous nature, with variation in size, shape, chemical composition, and surface charge. The most typical description of colloids concludes the particles are less than a few micrometers in diameter and larger than 1 nm (Ranville and Schmiermund, 1998; Buffle and Leppard, 1995), as can be seen in Figure 1.1. These particles are considered “permanently” suspended due to their extremely long settling times. Colloids can be settled with an increased gravitational field, consistent with the fact that they are not truly dissolved and that they form a stable two-phase system. In contrast, species such as humic substances, simple acids, and hydrated ions, are truly dissolved and form a single uniform phase. Particles slightly larger than 1 μm are considered particulates and form a non-stable two-phase system (Ranville and Schmiermund, 1998).

Colloidal particles exhibit a substantial increase in specific surface area as particles become smaller, as well as a greater degree of dispersion due to Brownian motion¹. When colloidal (sub-micron) particles travel in a subsurface environment, the size of the colloid in part determines the frequency of interactions with the immobile soil media. As particle size decreases, colloids have more random movement, which results in a higher collision frequency between them and the soil matrix. This can lead to size dependant sorption and desorption of the particles to the soil media. For particles larger than about

¹ Brownian motion describes random displacement of particles due to interactions with the media surrounding the particles. This is more thoroughly discussed in chapter 2.

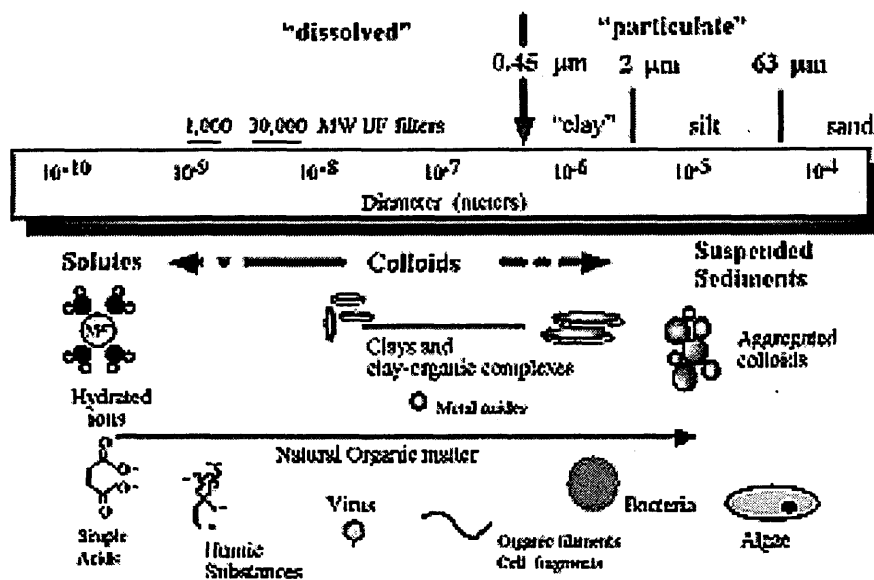


Figure 1.1 – Particle sizing of colloidal and particulates for natural waters. From Ranville and Schmiermund, 1998.

one micron, additional processes including straining by pores and gravitational settling, influence particle transport in groundwater.

Soil colloids are rarely exactly spherical in shape and are commonly found to be in the shape of rods and discs. This can pose a problem when trying to determine the behavior of the particle in a subsurface environment in groundwater. A particle can either have an increased or decreased transport capability through the media due to its shape. Another problem arises when attempting to analyze the size of non-spherical, polydisperse particles with conventional methods such as photon correlation spectroscopy (PCS), and single particle optical sensing (SPOS). These methods determine size through changes in light intensity, where a non-spherical particle may exhibit the optical properties of larger or smaller spherical particles. The particles have interactions with a beam of light that include refraction, polarization, reflection, and adsorption (Ranville and Schmiermund, 1998). These interactions with the light can potentially be used to determine the size and concentration of the colloidal particles. Directly examining the colloids through techniques such as scanning electron microscopy (SEM) allows for the investigation of particle shape. Use of automated image analysis techniques can also allow for the computation of size distributions. Another approach, the main subject of this work, is called field flow fractionation (FFF). This method separates the particles by their size and records the response from a ultra-violet (UV) detector. The time for the colloids to travel through the FFF channel is used to determine the size of particles. Non-spherical shape influences the results in that irregular particles travel differently than spherical particles of equivalent hydrodynamic diameter.

Another characteristic of colloidal particles is the chemical composition of each particle, which can vary significantly among particles of different sizes. The size of the particles can be especially relevant when surface coatings are present, which can alter the surface charge of the particle. The importance of surface coatings increases with decreasing size as a consequence of the greater surface to volume ratio of smaller colloids, which can influence the transport of materials such as heavy metals, radioactive

materials, biological entities (i.e. viruses, bacteria, etc) and organics that sorb to the surface coatings of iron or organic matter (Ranville et al., 1999; Kaplan et al., 1993). The composition of the colloids, especially surface coatings, directly influences the surface charge exhibited by the particles. The electrostatic charge of the particle, as well as the charge of the porous media in which the particle has contact, can determine the potential retention through adsorption or desorption (Elimelech et al., 2000). The bulk chemical composition of soil colloids is also highly variable between locations, for which soil type and depth in the profile are major influences.

Overall, there are two types of colloidal materials: hydrophobic and hydrophilic colloids. The hydrophobic colloids resist interactions with water and are mainly composed of mostly non-soluble materials. These tend to include most of the natural colloidal particles that are comprised of clays, precipitates, and aluminum, iron, and manganese (hydro)oxides. Hydrophilic colloids are soluble materials (i.e. organic matter, polymeric precipitates, etc) that form direct hydrogen bonds with water (Ranville and Schmiermund, 1998). Hydrophobic soil colloids are the focus of the research discussed in this thesis.

1.2 Colloid Transport Potential

Environmental colloids, as a result of their large specific surface areas and high degree of mobility in aquatic systems, play an important role in the transport of non-soluble contaminants by migration through porous media (Degueldre et al., 2000; Elimelech et al., 2000; McCarthy and Zachara; 1989). These contaminants include but are not limited to heavy metals, nuclear materials, and biohazards. McCarthy and Zachara (1989) describe the well-documented migration of plutonium and americium disposed at a liquid seepage site at the Los Alamos National Laboratory. The Defense program's scientists estimated that the radionuclides migrated up to 30 meters when pre-

disposal predictions, ignoring colloids, estimated the migration to be limited to a few millimeters from the site. In another example by McCarthy and Zachara (1989), plutonium and americium, deposited at another liquid outfall at Los Alamos, were detected over a mile from their deposition site. These radionuclides were shown to be present as colloids by ultrafiltration.

The basic principles of flow through a porous medium establish that diffusion to media surface and filtration of colloidal material may be responsible for removal of smaller and larger sized particles respectively, which is represented in Figure 1.2. At one point along the size distribution curve, there is an optimum size where the highest percentage of particles is transported through the porous medium. This preferred size for transport has been estimated to be at approximately 1 micron (Yao, Habibian and O'Melia, 1971). The colloidal transport mechanisms are shown in Figure 1.3, where small particles with Brownian movement interact through sorption and desorption with the media surfaces (B, C, and E). Larger particles are filtered out by sedimentation (A), or can be removed by filtration in pores, as represented by D (Ranville and Schmiermund, 1998). In addition to size, charge plays an important role in transport. The surface charge of the colloids is in part established by the bulk and surface composition of the particles (Elimelech et al., 2000).

1.3 Purpose of Project

One of the overall project goals was to compare a number of established and relatively new methods to characterize soils based upon their size. One of these methods, field-flow fractionation allows for the determination of size versus chemical composition. An additional objective of the work was to further investigate the ability of different types of FFF to accurately determine the size dependence of composition for soil colloids. The results of these investigations will allow future workers to study the effect

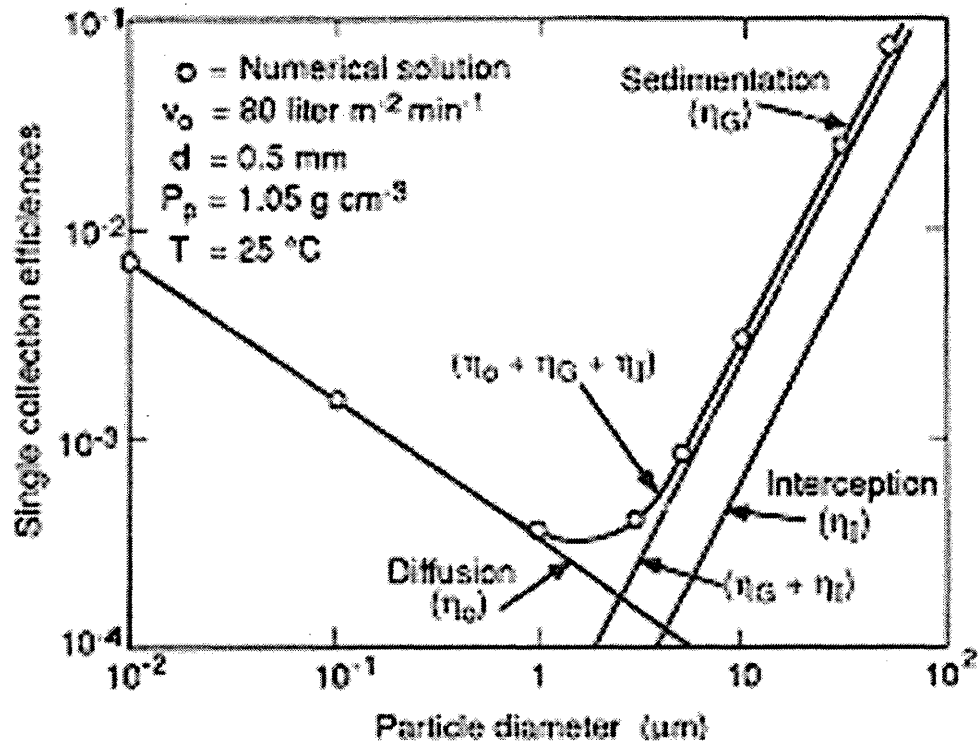


Figure 1.2 - Particle collection efficiencies of colloidal particles in a porous media. Smaller particles are diffused out with interactions with the media, where larger particles are filtered out. From Yao, Habibian and O'Melia, 1971.

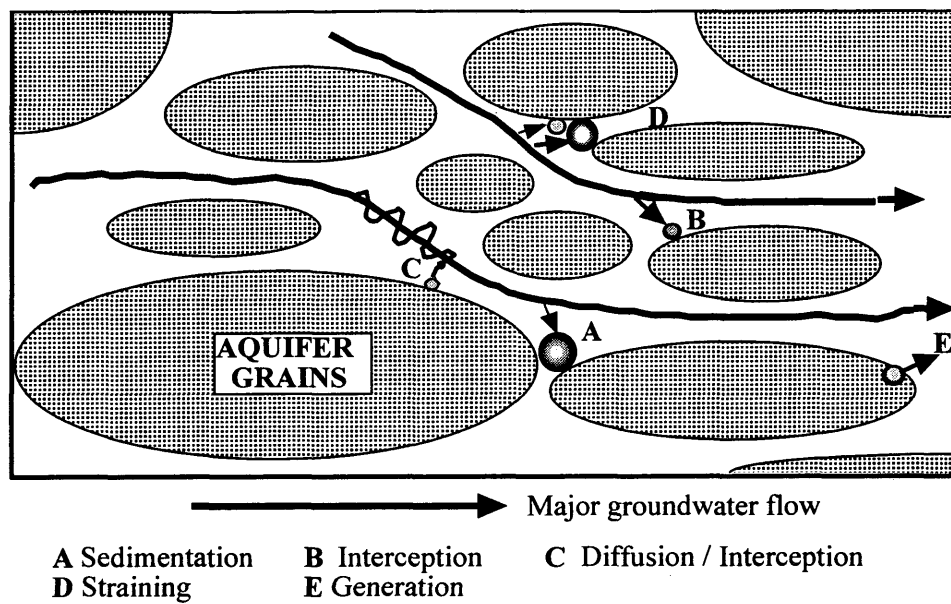


Figure 1.3 - Representation of colloidal transport mechanisms in groundwater through a porous media. Smaller particles diffuse more and have more interaction with the media surface. Larger particles are filtered out.

of the size and size-dependant composition on the transport of these colloids through a porous sand medium.

Historically, colloidal particles have been difficult to characterize, especially with respect to chemical composition versus size, due to limitations in many of the established size fractionation methods (i.e. filtration, centrifugation, etc). FFF is a relatively new chromatographic-like technique used to characterize and size fractionate soil colloids. Although FFF can in principle in a range of from a few nanometers to ten's of micrometers, a single FFF separation is generally limited to at most a 20-fold range in colloid diameter. Thus the colloidal material used in the study was extracted by ultrasonication and centrifugation into four size classes: $<0.2\ \mu\text{m}$, $0.2\text{-}0.8\ \mu\text{m}$, $0.8\text{-}2.0\ \mu\text{m}$, and $2.0\text{-}10.0\ \mu\text{m}$. Each fraction was thought to have a narrow enough range to be analyzed by FFF. The samples came from a surficial soil collected from Rocky Flats, which is contaminated with nuclear materials including plutonium. Actinides such as plutonium are highly insoluble and strongly sorb to particle surfaces. Thus particle movement may control actinide transport in the environment. The soils were size characterized using both sedimentation FFF (SdFFF), which generates an induced field through centrifugal force, and flow FFF (FIFFF), which generates an induced field by fluid flow. More commonly used size classification techniques were also applied and compared to FFF, including PCS, SPOS, and SEM.

When FFF is combined with elemental analysis by on-line coupling of inductively coupled plasma - mass spectrometer (ICP-MS), inductively coupled plasma-atomic emission spectroscopy (ICP-AES), or graphite furnace – atomic absorption spectrometer (GF-AAS), it provides a powerful means to investigate colloidal chemical composition versus size. Coupling of chemical analysis cannot be accomplished by other sizing techniques (i.e. SEM, SPOS, PCS, etc) as they simply size analyze without separation. The calculation of element ratios versus particle size allows for further interpretation of colloid mineralogy and the presence or absence of surface coatings.

1.4 Structure of thesis

This thesis establishes the two phases of the research project completed to fully characterize the natural soil colloids. The determination of particle size distributions of the colloids using various sizing technologies is fully discussed in Chapter 2. The main emphasis is upon a relatively new technique called field flow fractionation (FFF) and the comparison of these results to other particle sizing methodology such as SEM, SPOS, and PCS.

Chapter 3 reports the online and offline coupling of FFF to chemical composition instruments such as ICP-MS and GF-AAS. This demonstrates the potential for analysis of size versus chemical composition to determine if certain elements are size dependent in the colloids.

The final section, Chapter 4, is an overview of the other chapters' conclusions and provides discussion of potential future work.

CHAPTER 2

PARTICLE SIZING METHODS

2.1 Introduction

Determination of particle sizes, especially for submicron particles with large heterogeneity in size, shape, and composition, can be difficult due to the limitations of size-analysis techniques. A number of techniques have been developed to analyze fine particles and colloids, both polymeric or particulates, each of which having some associated assumptions and errors in common. Two common assumptions are that the colloids are spherical and have known, uniform densities. Some methods, including automated microscopic image analysis and single particle counting, detect individual particles and summation of the data result in number-based size distributions. Serial centrifugation or filtration, used with gravimetric or chemical analysis of collected fractions, provides mass-based size distributions. Assuming uniform density, mass-based distributions are also proportional to volume-based distributions. Field flow fractionation (FFF) with UV detection is the principal technique used in this research, and results from the ICP-MS experiments (Chapter 3) indicate that for the most part that mass (volume)–based distributions are obtained by this method. Light scattering methods such as photon correlation spectroscopy provide distributions that are based on the intensity of the scattered light, which can vary with particle size in a complex manner. It can be difficult to compare results obtained by number-based methods to those obtained by volume (mass)–based techniques.

In this study, soil colloids and fine particles (less than ten micron) were examined. Presently, the most commonly used size separation/analysis method for colloidal soil material employs high-speed centrifugation. This method is fairly accurate in the

separation of calculated size ranges if the effect of particle shape is taken into account and particle density is uniform. In addition, proper size separation requires multiple runs, which can have very long run times when dealing with small colloids (Chittleborough et al., 1992). The ultimate resolution (i.e. the narrowness of each size fraction) depends on the number of stages employed in the method. In most cases low resolution size distributions are obtained. Serial filtration, more commonly used for aquatic colloids, results in size separations based on the pore sizes of the filters used. Although it does not require knowledge of particle density, filtration suffers from a number of experimental artifacts (Buffle et al., 1995). Both of these methods, as well as FFF, not only provide size analysis but also a size-based separation. This allows chemical analysis of the fractions in order to determine of the effect of size on composition. The competing methods of image-analysis, particle counting, and light scattering do not provide separations and thus do not allow further investigation of colloid composition.

Flow field flow fractionation (FlFFF) and sedimentation FFF (SdFFF) are two sub-techniques of FFF that are capable of separation of particles based upon size and mass, respectively. Their greatest advantage over centrifugation and filtration is in their much higher resolution. Both methods are capable of accurately separating macromolecules, colloids, and particulate materials with sizes from 10^{-3} to 10^2 μm (Williams et al., 1996). These particles can include materials such as polystyrene beads, viruses, bacteria, and heterogeneous soil colloids. The high resolution of FFF, with its relatively short runs, and the addition of on-line element-specific detectors such as ICP-MS, make FFF a valuable tool for characterization of soils.

The specific objectives of the particle sizing section of the research were:

- 1) To size fractionate soil colloids from Rocky Flats into four sizes: 2-10 μm , 0.8-2 μm , 0.2-0.8 μm , and 10,000 Dalton to 0.2 μm .
- 2) To further size fractionate soils from objective 1 using FFF.
- 3) To compare FlFFF and SdFFF techniques for the two smallest colloid size fractions.

- 4) To analyze the size distributions of the soil fractions with other size analysis techniques and to compare with FFF results.

The first objective was used to reduce the polydispersity of the sample. This is necessary in order to perform FFF analyses under either normal-mode or steric mode conditions and to avoid a transition between modes during a given analysis. The modes of FFF operation are described below. The pre-fractionation step was also expected to improve the accuracy of the other size analysis methods.

2.2 Theory and Basis of Operation for Size Analysis Methods

In order to be able to fully assess the capabilities of the particle sizing methods, the mechanisms behind them must be understood. Depending on the technique, either the principles of Stokes law of settling or Brownian motion are the processes that govern the analysis. These two concepts and the specific particle sizing methods are described in detail in the following discussion.

2.2.1 Stokes Law of Settling

Stokes law of settling is an equation relating the terminal settling velocity of a smooth, rigid sphere in a viscous fluid of known density and viscosity to the diameter of the sphere when subjected to a known force field. It forms the basis of the serial centrifugation method and is the driving force that generates the field in the SdFFF technique. Assuming that the viscosity of the fluid is constant and soil particles are perfect spheres with the same density, the velocity of fall, V , can be obtained from equation 2.1:

$$V = \frac{2(\rho_s - \rho_w)}{9\eta} gr^2 \quad (2.1)$$

where ρ_s and ρ_w are the densities of the soil and the medium (in this case deionized water) respectively, η is the viscosity of the medium, g is the gravitational acceleration, and r is the radius of particle.

The calculation of the time, t , required for a particle with a certain radius, r , to settle a determined distance, h , can be expressed as:

$$t = \frac{18h\eta}{g(\rho_s - \rho_w)r^2} \quad (2.2)$$

Under normal gravitational conditions, g is equal to 1, which allows an effective size fractionation limit of about 1-2 micrometer. In addition, Brownian motion of colloids less than about one micron prevents settling under normal gravity and thus makes equation 2.1 invalid. Due to the ability of colloidal material to remain suspended in solution for long periods of time, an increase in g through use of a centrifuge greatly reduces the time necessary for settling and lowers the minimum radius for fractionation to less than 0.1 micrometers. The increase in g produced when using a centrifuge is dependent upon the rate of revolution (RPM) and the average radius of the centrifuge (r_{ave}) and can be expressed as:

$$g = \left[\left(RPM * \frac{6.283}{60} \right)^2 * \left(\frac{r_{ave}}{9.8} \right) \right]^2 \quad (2.3)$$

These equations, assuming a particle density of 2.5 g/cm³ can be used to calculate the times required to obtain the desired size cuts for the prefractionation using serial centrifugation.

2.2.2 Brownian Motion

Brownian motion is the observed movement of small particles as the molecules of the surrounding medium randomly bombard them. This bombardment of a particle with the medium causes erratic displacement of the particle. The erratic behavior of a particle makes it impossible to determine the number of collisions it may encounter with other particles. The theory predicts though, the smaller the particle, the more it will be influenced by the media into more erratic displacement and have a greater potential of interaction with other particles. The magnitude of this erratic motion is formally described by the diffusion coefficient of the particle. Several techniques determine particle size based on the magnitude of the diffusion coefficient. These methods include photon correlation spectroscopy (PCS) and normal-mode elution of both SdFFF and FIFFF. This is described in more detail in the discussion of each of these techniques.

2.3 Particle-Sizing Methods

Techniques utilized in this study for the high-resolution analysis of colloidal material include: Single Particle Optical Sensing (SPOS), Scanning Electron Microscopy (SEM) with automated image analysis, Photon Correlation Spectroscopy (PCS), and both sedimentation and flow FFF methods. These methods are discussed briefly below.

2.3.1 Single Particle Optical Sensor (SPOS)

The specific SPOS instrument used, developed by Particle Sizing Systems (PSS), was the AccuSizer 780. The SPOS method provides a particle size distribution by quickly sizing and counting large numbers of particles, one at a time. A light source with a wavelength of 720 nm illuminates the particles as they pass through a quartz capillary.

Two photodiode detectors are used in combination to measure both light blockage and light diffraction by each particle. The light-blockage sensor is directly in line with the laser, whereas the scattering sensor is located at an angle of approximately 25 degrees. The combination of signals from the two detectors results in a linear millivolt response versus particle diameter over a size range of 0.4 to 500 micrometers. This calibration curve was obtained by using polystyrene microspheres of known diameters (Duke Scientific). The instrument extracts up to 20 mL from a reservoir containing a very dilute concentration of the sample particles by use of an automated syringe. Counting particles and determining their size as they flow through the light cell generates a number-based size distribution. The measurement process was repeated two additional times and the particle size distribution in the total volume of sample extracted was computed.

SPOS is very fast, efficient, and provides a number-based particle size distribution that can be accurate. The method does not rely on either settling or Brownian motion. From the distribution, it is possible to translate the number distribution into a cross sectional area or volume distribution with relative ease.

The effectiveness of SPOS in determination of particle sizing also has limitations associated with it. Concentrations of particles injected into the instrument must be very dilute in order to avoid the problem of coincidence. Coincidence occurs when two particles are sized simultaneously. This results in an underestimate of particle number and an overestimate of particle size. Thus low particle concentrations (generally $< 10^4$ particles/ml) are required, so calculation of the initial concentrations of particles requires careful measurement of the dilution factors used. Effective size analysis yields distributions of particles as large as 500 micron and as small as 0.5 μm . This lower limit leads to a large number of particles in environmental samples being unanalyzed. SPOS is able to only size particles; separation into size fractions for further analysis of the colloids is not possible. The most complicated problem is that the calibration curve is generated using spherical particles, most commonly polystyrene microspheres. Non-spherical shaped particles, or particles with optical properties different from polystyrene, yield

variable results and can lead to erroneously reported sizes. An additional problem arises in converting the measured number distributions into volume (mass) distributions. For the upper range of the size distribution particle numbers are low but these few particles dominate the volume distribution, making this portion of the distribution “noisy”. In this study, this problem was somewhat reduced by arbitrarily rejecting the upper five percent of the number distribution prior to computing the volume distribution.

2.3.2 Photon Correlation Spectroscopy (PCS)

The PCS method is based on the measurement of the diffusion coefficient of the sample particles. The instrument used was the Brookhaven Zeta Plus, which has a laser with wavelength of 632 nm. A detector located at 90 degrees to the laser detected the light scattered from the sample particles. The basis of the technique depends on measuring the rate at which the scattered light intensity changes, by determining an “auto-correlation function”. In simple terms, the light reaching the detector results from the combination of constructive and destructive interference of the light scattered off of ten’s of thousands of particles in the sample volume illuminated by the laser. If the particles are small they are rapidly moving randomly in solution. Thus between any short increments of time their relative positions will have changed greatly. Thus the combined interference patterns will also change and result in a significant change in the light intensity reaching the detector. For larger particles, their movement is less, and thus the intensity of light reaching the detector will also change less over short periods of time. Thus a method exists to determine the size of the particles from the changes in scattered light intensity over short periods of time (milliseconds). For best results, samples are needed that are similar in size, shape, and refractive index. These are perhaps impossible limitations when evaluating environmental samples.

Although complex mathematical algorithms exist that can be used to fit data from polydisperse samples to create a size distribution, only mean size was examined in this study. The results from the PCS for a sample containing high variability appeared to produce a mean value, which is skewed toward the size with the most particles (i.e. the smaller sizes). This seemed to neglect larger particles that contributed more mass and volume, but had smaller number concentrations. In environmental samples, a larger number of small particles will skew the results towards the smaller end. Another limitation of the PCS is that sample concentrations must be dilute, although not as dilute as SPOS. High turbidity of the solution will limit the effectiveness of the method. While there are quite a few limitations of using the PCS, there are also benefits. Minimal alteration of the sample is generally required. The method is gentle and aggregation is most likely not disturbed. Homogeneous samples such as hematite produce favorable results. Finally, reproducibility is high and analysis time is short.

2.3.3 Scanning Electron Microscopy (SEM)

SEM was originally developed in the early nineteen-sixties and has since become a valuable tool for analyzing particles and their surfaces. It has been evaluated in many other studies and thus will only be described briefly. The SEM uses a lens condenser to concentrate a beam of electrons from an electron gun in order to scan particles. The electrons that are scattered by the particle are collected by a Faraday cage, which produces a signal that alters the brightness of a cathode ray tube display. The tube is then scanned by with an incident beam to generate a surface image of the specimen. The SEM is able to supply information on surface topography, bulk microstructure, quantitative studies, and crystallographic information (Tadjiki, 1999).

The generation of images is possible with SEM, which is different from most other particle sizing methods. Shapes of the particles can be studied, as well as the surface of the particles.

While it is possible to view and size particles, SEM requires long times to view a statistically significant number of particles, and is fairly expensive to run samples. It is also not possible to conduct chemical analysis of the particles beyond qualitative elemental analysis of coatings and other surface phenomena. Use of SEM for particle size analysis has been facilitated by the use of automated image analysis techniques (Seaman, 2000). These methods allow for the counting of several thousand particles per sample in order to develop number-based size distributions. As is the case with any particle counting method, the conversion to volume (mass) distributions results in a very noisy signal at the larger end of the distributions. This is especially true for very fine colloid fractions.

2.3.4 Field Flow Fractionation (FFF)

There are numerous FFF separation methods that have been developed using the theory behind FFF, however, the two that are most applicable to environmental colloids are sedimentation FFF (SdFFF) and flow FFF (FIFFF). Both the SdFFF and FIFFF instruments, manufactured by FFFractionation, LLC (Salt Lake City, UT), operate based upon the principle of an applied perpendicular force field that concentrates particles against an accumulation wall in a thin, parallel-walled channel. Through a variety of forces such as Brownian motion, hydrodynamic lift forces, or particle size, the particles are transported away from the accumulation wall. A parabolic shaped laminar flow velocity distribution (see Figure 2.1) separates the particles in a flow of carrier fluid of particle-free water containing a surfactant (0.001% to 0.1% FL-70 was used in this

experimentation) and sodium azide (0.01%). A centrifuge creates the applied gravitational field in the SdFFF, whereas the FIFFF field is created with a cross-flow¹.

The FFF channels are comprised of a thin ribbon-like channel that have a thickness, w , of approximately 0.22 mm and a breadth, b , of approximately 2 cm. The length of each channel, L , is variable depending on the type of instrument. The FIFFF has a channel length of 27.2 cm, where the SdFFF has a length of 93.7 cm.

Method development to determine optimum conditions for particle elution in FFF technologies is conducted with polystyrene bead standards, which is a time consuming process. Once a method is determined to accurately determine the size of the polystyrene beads, the established conditions have a high probability of accurately measuring the size of the soil particles.

The instruments operate under two conditions of particle elution, either normal or steric mode. Normal mode is represented in Figure 2.1 where the smaller particles elute first due to their larger diffusion coefficients. Brownian motion causes the smaller particles to diffuse away from the wall and thus they interact with the higher flow. The larger particles have smaller diffusion coefficients and do not diffuse as far from the accumulation, therefore elution occurs later. Under steric conditions, larger sized particles are hydrodynamically lifted off the accumulation wall, allowing the larger particles to elute before the smaller particles. These two elution modes are described in more detail in the following discussion.

A particular problem in characterizing natural soil colloids arises when the particles are not spherical in shape. Shape effects will influence the measured size of the particles, either causing them to elute earlier or later than theory predicts. For instance, a rod or plate shaped particle may elute out of the channel at the same time as a much larger spherical particle in normal mode.

¹ Cross-flow is a transverse flow through a semi-permeable membrane that creates an applied field. This applied field concentrates injected particles along the accumulation wall, where forces such as Brownian motion counteract the applied field to equilibrate the particles at a particular height in the laminar flow through the channel.

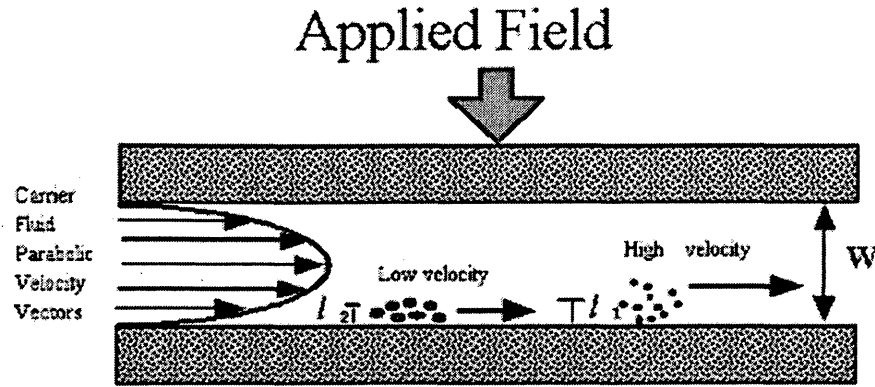


Figure 2.1 - Representation of particle separations through an FFF channel using normal mode. Larger particles are diffused away from the accumulation wall less than the smaller particles and therefore the large particles are held in a lower flow velocity. Surface resistance creates a parabolic flow.

2.3.4.1 Normal Mode Elution

Separations of particles in the FFF channel occur with particles diffusing into various heights above the laminar (channel) flow. When a steady state occurs, the particle concentration, $c(x)$, at a distance, x , from the accumulation wall can be expressed as:

$$\frac{c(x)}{c_0} = \exp\left(\frac{-x}{\ell}\right) \quad (2.4)$$

where c_0 is the particle concentration at the accumulation wall and ℓ is the average height where particles of similar size are concentrated. The estimation of ℓ for similarly-sized particles can be expressed as:

$$\ell = \frac{D}{|U|} \quad (2.5)$$

where D is the diffusion coefficient and U is the field-induced velocity in the x direction, which is perpendicular to the laminar flow. If a species is strongly affected by the U , then the height, ℓ , from the accumulation wall is going to be small. With a smaller U , diffusion from the accumulation wall will be greater. The field-induced velocity in the x direction, U , is proportional to the field strength and depends on the type of field used.

The diffusion coefficient is represented by the Stokes-Einstein equation:

$$D = \frac{kT}{3\pi \cdot \eta \cdot d} \quad (2.6)$$

where kT is representation of the thermal energy (k is the Boltzmann constant and T is the absolute temperature), η is the fluid viscosity, and d is the diameter of the spherical particles.

Basic theory of FFF retention assumes a steady-state in the laminar carrier flow and the velocity of the local carrier fluid, $v(x)$, can be expressed with:

$$v(x) = 6 \langle v \rangle \left[\left(\frac{x}{w} \right) - \left(\frac{x}{w} \right)^2 \right] \quad (2.7)$$

where w is the channel thickness and $\langle v \rangle$ is the mean fluid velocity. Due to the parabolic nature of the flow, the maximum flow at the center channel ($x = w/2$) is 1.5 times that of the $\langle v \rangle$.

The retention ratio, R , which is the delay of the particles over the eluent, can be expressed as:

$$R = \frac{t^o}{t_r} \quad (2.8)$$

where t^o is the average residence time of the eluent and t_r is the average residence of the particles. The greater the time difference the lower the retention ratio. If the carrier flows are constant the retention ratio can be expressed as:

$$R = \frac{V^o}{V_r} \quad (2.9)$$

where V^o is the void volume of the channel and V_r is the retention volume of the particles.

A simplified expression for the mean particle migration velocity over the entire channel thickness can be described as

$$R = \frac{[c(x)v(x)]}{[c(x)][v(x)]} \quad (2.10)$$

where $\langle c(x) \rangle$ and $\langle v(x) \rangle$ are the mean concentrations of the particles and mean fluid velocity respectively. When substituting equations 2.4 and 2.7 into 2.10, we obtain

$$R = 6\lambda \cdot \left(\coth\left(\frac{1}{2\lambda}\right) - 2\lambda \right) \quad (2.11)$$

where λ is the retention parameter or dimensionless thickness of the sample cloud ($\lambda = \ell / w$). For small λ and ℓ values, equation 2.12 can be rewritten as

$$R \approx 6\lambda \quad (2.12)$$

2.3.4.1.1 Flow FFF Theory

FFF theory for FIFFF dictates that particles are separated based upon their diffusion coefficients (Schimf et al., 498), which inversely related to the diameter, d , of the

particle. Thus the retention parameter of the particles increases as the diffusion coefficient increases, which can be represented in the equation:

$$\lambda = \frac{DV^0}{V_c w^2} \quad (2.13)$$

where V_c is the cross-flow, V^0 is the channel flow, and w is the channel thickness. Substituting the Stokes-Einstein equation (2.7) into equation 2.14 yields

$$\lambda = \frac{kTV^0}{3 \cdot \pi \cdot \eta \cdot V_c w^2 d} \quad (2.14)$$

which demonstrates the inverse relationship between λ and d . The smaller a particle is in size, the higher the diffusion coefficient is, which carries the particle higher into the parabolic flow. This in turn elutes the particle sooner than a particle nearer the accumulation wall. Rearranging equation 2.15, it is possible to determine the hydrodynamic diameter associated with an established height in the channel flow, expressed as:

$$d = \frac{kTV^0}{3 \cdot \pi \cdot \eta \cdot V_c w^2 \lambda} \quad (2.15)$$

So a general relationship used between d and λ can be expressed as:

$$R \approx 6\lambda \approx t_o / t_r \quad (2.16)$$

The inverse relationship of λ and t_r in equation 2.16 demonstrate that when applied to equation 2.15, t_r and d are directly proportional. In order to obtain a mass-based size distribution, $m^c(d)$, the detector response, S_i , is transferred to relative amount using the following equation:

$$m_i^c(d) = \frac{S_i}{\sum S_i} \cdot \frac{\Delta t_r}{\Delta d} \quad (2.17)$$

where i represents the i 'th point and Δt_r is the fixed elution time corresponding to the time interval (Schimpf et al., 2000). This accounts for the generally non-linear relationship between time and diameter.

2.3.4.1.2 Sedimentation FFF Theory

Separation of particles in an SdFFF channel occurs with the application of an increased gravitational field generated with a centrifuge and a transverse flow through the channel. Since a gravitational field is required to produce an applied field, the separation of particles is mass dependent and calculation of particle size requires a known density. The retention parameter for the SdFFF can be expressed as:

$$\lambda = \frac{6 \cdot k \cdot T}{\pi \cdot d^3 \cdot \Delta \rho \cdot S \cdot w} \quad (2.18)$$

where $\Delta \rho$ is the difference in density ($\rho_s - \rho_w$ where ρ_s is the density of the particles and ρ_w is the density of the water) and S is the acceleration due to gravity or centrifugation. This can best be expressed as

$$S = \omega^2 r_0 \quad (2.19)$$

where ω is the angular velocity and r_0 is the radius of the channel. Like the FIFFF, the retention of the particles in the channel of the SdFFF is directly proportional to the diameter of the particle, as represented in equations 2.16 and 2.18. The SdFFF can be programmed to have higher resolution at the beginning of the run, and less resolution at

the end of the run. This is achieved through a power program feature, where the field strength is varied during the run by slowing the centrifuge.

2.3.4.2 Steric Mode Elution

Steric mode elution occurs when a particle exceeds in size the value of its calculated cloud thickness ($\lambda = \ell / w$). With this large size, the center of the particle is higher than its calculated vector in the parabolic channel flow, which then elutes the particle too soon. The retention of the particles can be represented with:

$$R = 6 \cdot (\alpha - \alpha^2) + 6\lambda \cdot (1 - 2\alpha) \cdot \left[\coth\left(\frac{1 - 2\alpha}{2\lambda}\right) - \frac{2\lambda}{1 - 2\alpha} \right] \quad (2.20)$$

where α is a dimensionless unit to analyze the particle radius, a , of a solid sphere that is too large for its proper low velocity vector. It can be analyzed using the following equation:

$$\alpha = \frac{a}{w} \quad (2.21)$$

When both α and λ are small, the result is:

$$\lim R = 6 \cdot \alpha + 6 \cdot \lambda \quad (2.22)$$

This equation, however, assumes that the particle moves at the velocity of the fluid at the center of the gravity of the particle. This neglects some of the hydrodynamic forces occurring when the particle is near the accumulation wall, such as particle rotation and viscous drag (Martin and Williams, 1992). By modification of the equation and addition of a velocity correction factor, γ , the retention ratio can be expressed as:

$$R = 6\gamma \cdot \alpha \quad (2.23)$$

assuming $\lambda \ll \alpha$.

2.3.4.3 Representation of the Data

The data that is collected from each FFF run can be plotted and characterized as a fractogram. A fractogram is a plot of detector response versus time or elution volume as shown in Figure 2.2a. The response can be UV absorbance, ICP-MS ion current, atomic absorption, or any other instrument. From the fractogram, plots of particle size or molecular weight distributions can be obtained as seen in Figure 2.2b, which is a plot of corrected detector response versus computed diameter or molecular weight from either FFF equations or a calibration curve. The correction of the detector response is described in equation 2.17.

2.4 Experimental Design

The main goal of the experiment was to test the effectiveness of the SdFFF and FIFFF techniques against other particle sizing techniques for environmental colloids. In order to do this, colloidal material was collected from a soil and separated into four size fractions. The separation of the soils and the experimental setup of the FFF techniques are described in more detail in the following narrative.

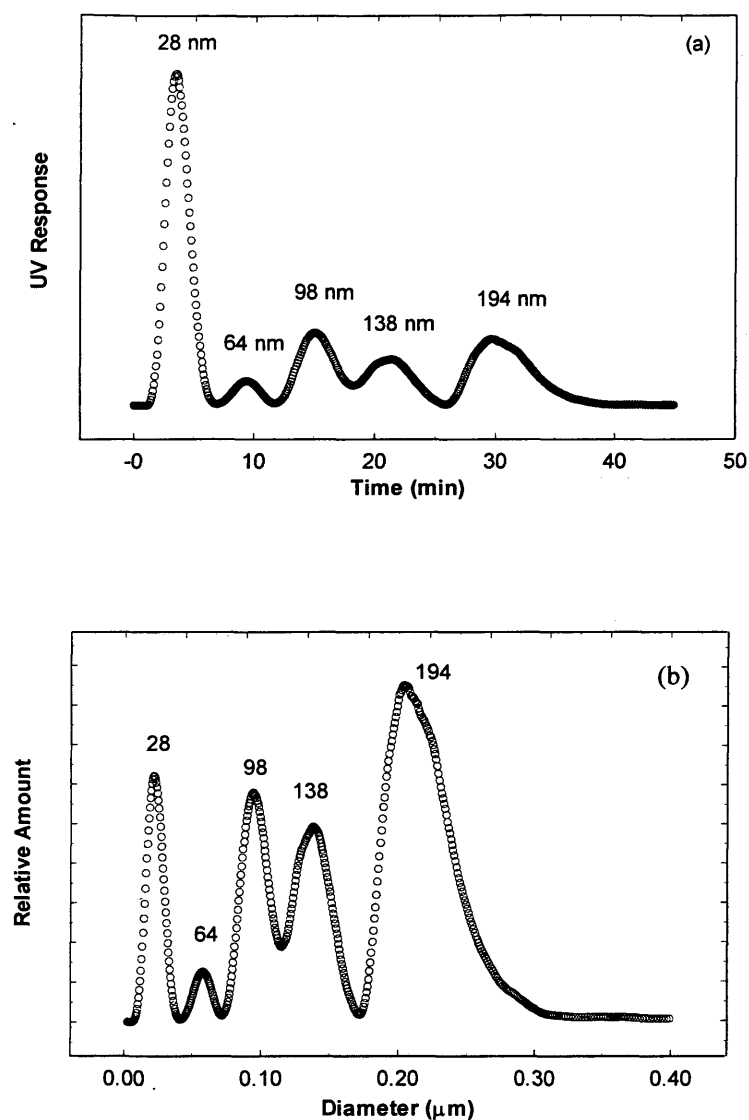


Figure 2.2(a,b) – Normal mode elution FIFFF run of five polystyrene beads displaying (a) the fractogram with UV response plotted against time and (b) converted size distribution of relative amount versus diameter.

2.4.1 Soil Preparation

Colloidal (less than two micron) and fine silt (2-10 micron) material was isolated from a soil sample collected from the upper five centimeters of the soil surface at the Rocky Flats Environmental Technology Site, a former nuclear weapons production facility, which is located near Denver, CO. Initial preparation of the soil included wet sieving the soil to less than 0.2 mm. A total of 64.0 g of the less than 0.2 mm soil mass was used from three separate surficial soil samples (14.7, 24.3, and 25.0 g), which can be characterized as a clay-loam soil type. The soil was dispersed in 150 mL of deionized water and the soil aggregates were mechanically dispersed by ultrasonication. A Fisher Scientific 550 Sonic Dismembrator was used for 15 minutes to disrupt the aggregates that were present. Prefractionation of the material consisted of settling and centrifugation, which was used to generate five size fractions, the four smaller fractions being the focus of the research.

Following the initial sonication of the whole soil, pre-washing of the soil material with nano-pure water was used to separate the larger sand and coarse silt particles from the smaller suspended material. The suspension was shaken, allowed to stand briefly and the suspended material is then decanted. The process was repeated several times to collect the suspended material, which was placed in a one liter-graduated cylinder. The suspension was allowed to settle for one hour. The upper 28 cm, which gave a volume of 760 ml, was then pumped off using an HPLC pump. Using Stokes Law of Settling, it was computed that particles greater in size than ten micron had settled. The larger particles at the bottom of the cylinder were washed several times to extract the colloidal material by repeating the settling procedure after addition of new water to the cylinder. The solution that was decanted off was then re-sonicated for 30 seconds to break the bonds of aggregated particles. The suspension was then permitted to settle approximately 24 hours in order to obtain a two-micron size cutoff. The settling process was repeated three times, in order to separate the 2-10 micron soil from the less than two-millimeter

soil. Each time this process yielded approximately 760 mL of sample. The re-washing ensures collection of colloidal material near the two-micron size distribution.

2.4.2 Prefractionation by Centrifugation

The less than 2 μm sample was distributed evenly into 250 mL centrifuge bottles, of which three further size fractions were desired, less than 0.2 μm , 0.2-0.8 μm , and 0.8-2 μm . A Marathon 12 KBR centrifuge by Fischer Scientific, which operates as a swing-out rotor centrifuge, was used to fractionate the soils. Centrifugation of the sample was then commenced for a pre-determined time according to Stokes Law of Settling for each size class, using the calculated gravitational forces of the centrifuge. For the initial size cut of 0.8 μm , the centrifuge was spun at 3000 RPM for 22 minutes. The upper 6.5 cm of the solution was then extracted using a HPLC pump and placed in the centrifuge once more for 155 minutes at 4500 RPM to separate the two smaller size fractions. The less than 0.2 micron solution, the solution remaining after the latter centrifugation, is then recombined with the 0.8-2 micron sample and centrifuged at the same gravitational force and time to re-separate the 0.8-2 micron sample. This is done to wash less than 0.8 micron particles from the 0.8-2 micron fraction, without greatly increasing the volume. The process is completed twice without the addition of new water, and three times with the addition of new water. The resulting less than 0.8 micron fraction was then re-centrifuged at the higher g force to complete the separation of the less than 0.2 and 0.2-0.8 micron fractions. The less than 0.2 micron size fraction was filtered through a 10,000 Dalton Milli-Pore filter. The material on the filter was recovered and represented the 0.2 to approximately 0.01 micron size fraction.

2.4.3 FFF Setup

Various FFF methods exist for particle separation. Each method is centered on which type of FFF channel and field is used for particle separation. The two most commonly utilized for environmental colloidal separations are the SdFFF and the FIFFF, which were both utilized for this study.

2.4.3.1 FIFFF Design

The FIFFF channel applies a force using a transverse flow through a semi-permeable membrane to create its applied field. The setup design (as shown in Figure 2.3) contains two independent HPLC pumps: one for the channel flow, and one for the cross-flow, the latter is controlled with a computer. For most of the FIFFF runs, the cross-flow rate was decreased during the separation, generally in a linear manner.

The channel flow first flows through a valve control interface that places the pump in a loop. The solution can either flow through the channel, or can bypass it, which allows for an equilibration of the particles. From the valve control, the solution is then directed to the injector loop to inject the sample, which is then carried to the channel. Upon exiting the channel, a UV detector records the response in the increased refraction of light (which is established at 254 nm) after it passes through a needle valve that is used to regulate the exiting flow. From here, the solution can either be carried off to waste, be coupled online to chemical composition technology such as ICP-MS, or be collected in a fraction collector for offline analysis with technology such as a GFAAS.

The computer is essential for collecting the data (i.e., time, UV response, and cross-flow) and regulating the flow of the cross-flow. In more complicated setups where a decreasing cross-flow is needed through the duration of the run, the cross-flow is placed in a large loop with a bubble-trap. Decreasing pressures with decreasing flows make it

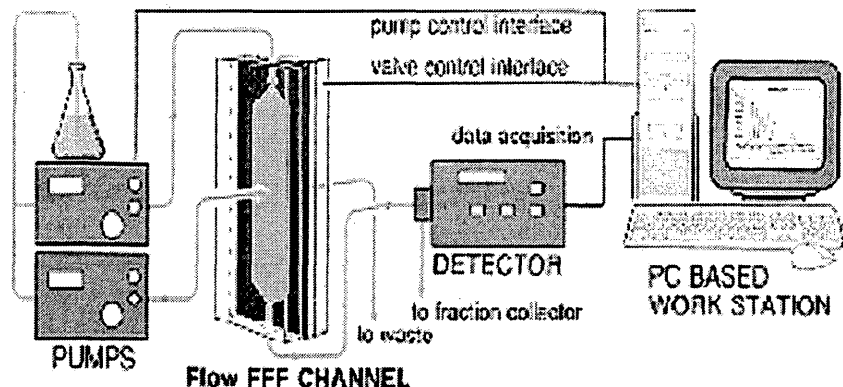


Figure 2.3 – Experimental design setup of an FIFFF channel. From FFFractionation website (www.fffractionation.com).

impossible to regulate the flow if not placed in this loop. By placing the flow into a loop, however, it is impossible to determine the actual cross-flow and therefore must assume the pump's accuracy. The cross-flow is also placed in a loop that can bypass the channel (needed to clear the channel of retained particles on the membrane) or flow through the channel.

The channel itself is made of ceramic inside a clear block. The channel has an area of approximately 54.3 cm^2 and a variable thickness, which is dependent upon the spacer, membrane, and amount compaction from the bolts holding the two halves of the block together.

2.4.3.2 SdFFF Design

The SdFFF is an instrument that uses a gravitational or centrifugal field to create an applied field upon particles in a circular channel. The basic layout of the SdFFF is shown

in Figure 2.4. The channel flow through the SdFFF originates from a carrier reservoir through an HPLC pump, which then flows through a valve control interface to allow flow through the channel or divert directly to waste. The injection port introduces the sample to the channel, which has an area of 187.5 cm^2 with a calculated void volume of 4.2 mL and an approximate thickness of 0.0224 cm. The centrifuge itself is where the separation occurs by creating an applied field through an increased gravitational field. Upon exiting the system, a UV detector records a response in the increase in refraction of the light. From here, the setup is similar to the FIFFF in that the flow can be diverted to waste or to other instruments for chemical analysis. This can include a direct coupling to an ICP-MS for online chemical and size analysis, or a fraction collector for offline analysis to an instrument such as a GFAAS. A computer is responsible for data collection and controlling the speed of the centrifuge.

2.5 Results and Discussion

Each of the methods discussed earlier were utilized to analyze the size of Rocky Flats soil. The results are presented below.

2.5.1 Centrifugation

The mass of the colloidal and fine silt material was determined from the concentration of particles in each of the size fractions of Rocky Flats soils. Approximately one milliliter of each sample was collected and dried for 72 hours in glass vials at 50°C to ensure the soil material was thoroughly dried. Weight measurements were conducted before and after the drying process. There was negligible loss of weight by the glass vial, verified through experimentation. The total mass in each fraction was

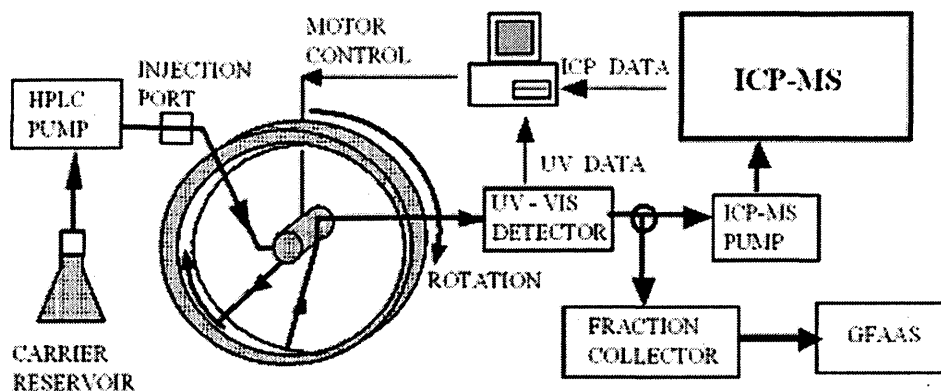


Figure 2.4 – Experimental design of the SdFFF channel depicting potential coupling of chemical analysis instruments such as ICP-MS and GFAAS.

calculated based on the mass per milliliter times the volume of each fraction. Table 2.1 represents the percent mass in each of these size fractions. As can be seen, most of the mass is present in the two largest size fractions, and represents nearly 80 percent of the colloidal and fine silt material. With an initial mass of 64.0 g soil of particles less than 0.2 millimeter, the total amount of colloidal and suspended material less than ten micron is about ten percent of the soil sample.

Table 2.1 - Bulk size distribution of Rocky Flats soils with representation of total mass in each size range, percent represented of the mass less than 10 μm , and percent of total initial soil less than 0.2 mm.

	Diameter			
	10-2 μm	2.0-0.8 μm	0.8-0.2 μm	<0.2 μm
Mass	2.599	2.696	1.049	0.157
% Mass <10 μm	40.0	41.5	16.1	2.4
% Total of Soil	4.1	4.2	1.6	0.25

2.5.2 SPOS

The SPOS was used to generate particle size distributions for the two largest size fractions of the Rocky Flats soils. It's detection limit of about 0.5 micron prevented SPOS measurements of the two finer fractions. From the data, number and volume distributions were generated to represent the composition of colloidal matter in the sample. As shown in the following figures, logarithmic scales present the data more clearly.

Figure 2.5 illustrates that most of the particles are smaller than two micron, as expected in the 0.8-2.0 micron soil fraction, with a minimal number of larger particles. These larger particles, however, translate into a large fraction of the volume distribution. If the effects of the few larger particles are ignored, the volume and number distributions peak at approximately 1.12 μm and 0.61 μm respectively. The results are in good agreement with the predicted size cuts based on the Stokes settling calculations.

The 2.0-10 micron fraction of soil, represented in Figure 2.6, illustrates that the majority of the particles are still sub-micron with a peak of approximately 0.54 μm when analyzing the number distribution. The volume distribution, however, shows that the larger particles constitute a greater percentage of the particle mass, with a peak at approximately 5.96 μm .

As seen in Figures 2.5 and 2.6, the volume distributions more accurately represent the size estimates determined through Stokes Law of Settling for the fractionated samples. This is expected as the sedimentation size cuts are based on mass obtained in each fraction, which should be roughly proportional to the volume distributions, assuming no major differences in density occur in the different size fractions.

2.5.3 PCS

Through the course of the experimentation, PCS was determined to be an ineffective method in particle sizing of natural soil colloids due to their heterogeneous nature. Table 2.2 lists the mean sizes determined from triplicate runs with each run having ten measurements. Although the PCS results are consistent with the calculated size cuts for the smallest size fraction, the PCS results are much smaller than predicted based on the size cuts of the larger fractions. The relatively poor results for PCS should be further investigated if PCS can be considered as a viable technique for environmental colloid characterization.

Table 2.2 - PCS mean data size of Rocky Flats soil fractions.

Size Class	Mean Size (μm)
<0.2 μm	0.16
0.2-0.8 μm	0.28
0.8-2.0 μm	0.35
2.0-10.0 μm	0.45

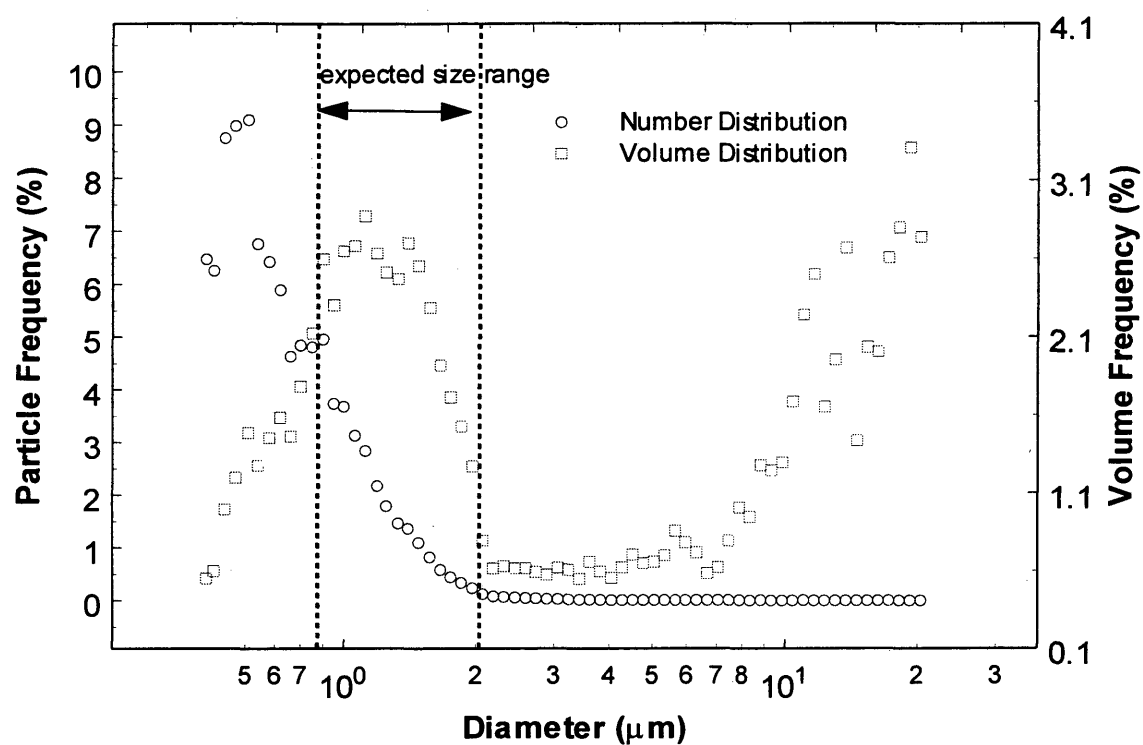


Figure 2.5 – SPOS analysis of the 0.8-2.0 μm fraction of Rocky Flats soils. Number and volume distributions of the data are plotted on a logarithmic scale.

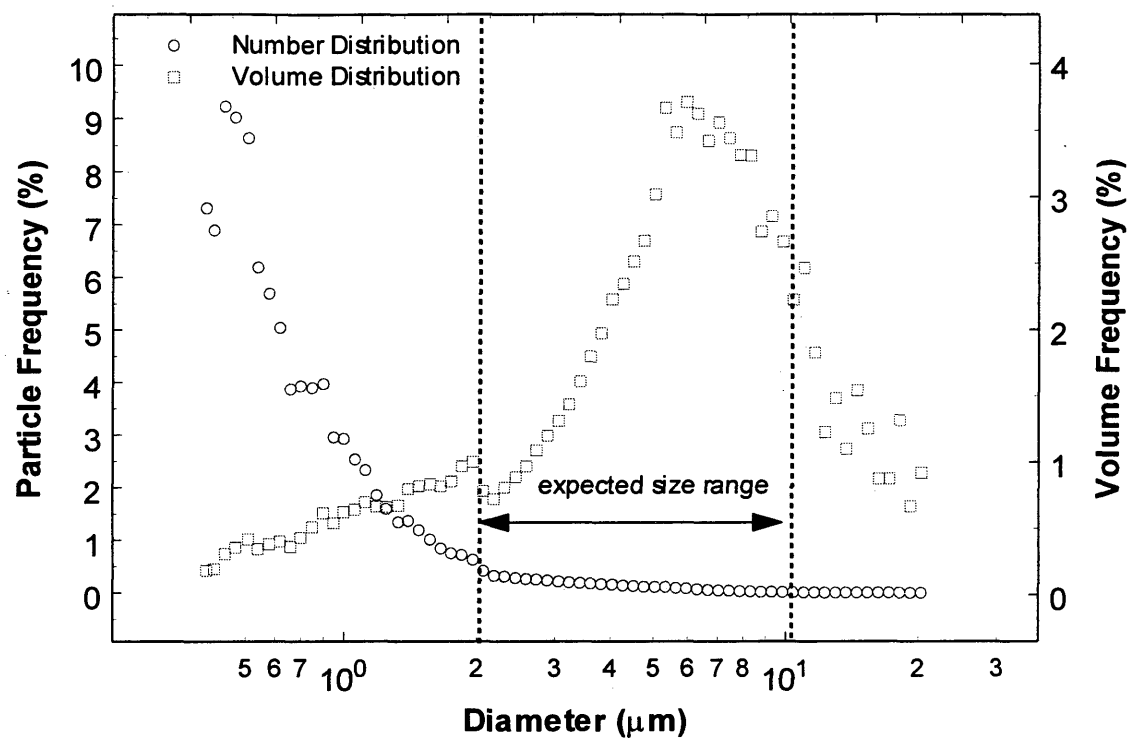


Figure 2.6 – SPOS analysis of the 2.0-10 μm fraction of Rocky Flats soils. Number and volume distributions of the data are plotted on a logarithmic scale.

2.5.4 SEM

The colloidal material of the four fractions was analyzed through a series of SEM experiments. Particle size distributions representing both number and volume distributions were generated for each of the experiments. Due to very small numbers of particles having a great effect upon the volume, five percent of the larger particles were removed from the calculations. The majority of these are very large particles that skewed the results of the SEM, especially the volume distributions.

The less than 0.2 micron size fraction, as shown in Figure 2.7, is highly skewed to the smaller sized particles for the number distribution, but is more scattered and favors the larger particles on the volume distribution with a continual increasing trend. Even with five percent of larger particles removed, the few remaining large particles create a highly scattered volume distribution. A total of 1383 particles are represented in the figure, of which 77.3 percent are less than a half-micron in diameter, but only represent 2.35 percent of the volume.

Figure 2.8 represents the 0.2-0.8 micron size fraction. Similar to the smallest size fraction, the majority of the particles are in the smaller size range. There is a sharp increase around 0.2 micron in the number of particles, with the majority of the particles smaller than 0.7 micron, as would be expected. The volume distribution follows the trend, but a few larger particles skews the results to the larger particle sizes. With a total of 1845 particles represented in the figure, 99.7 percent of the particles are less than one micron, but represent only 80.4 percent of the volume.

Like the two smaller fractions, the 0.8-2.0 micron soil fraction contains a majority of its particles in the sub-micron range, as illustrated in Figure 2.9. Approximately 77 percent of the particles are less than 0.8 micron in diameter, with a peak in the number distribution around 0.5 micron. The volume distribution for this fraction is linear, until the volume reaches approximately 1.6 micron, after which the points are fairly scattered. The linear portion of the analysis represents 95.5 percent of the particles, while only 67.7

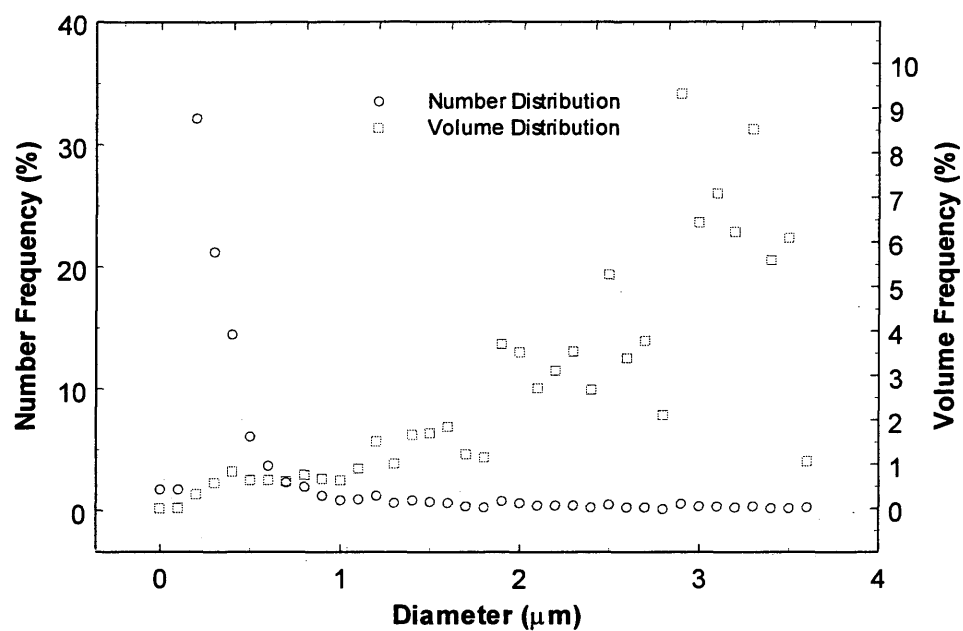


Figure 2.7 – SEM experimental results of the <0.2 micron Rocky Flats soil fraction, with both the number and volume distributions calculated.

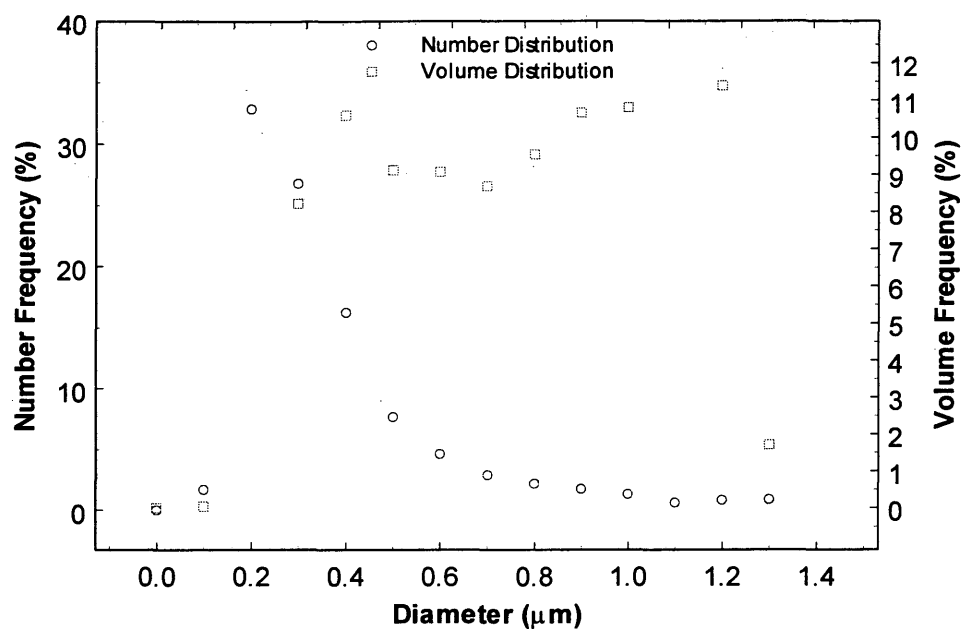


Figure 2.8 – SEM experimental results of the 0.2-0.8 micron Rocky Flats soil fraction, with both the number and volume distributions calculated.

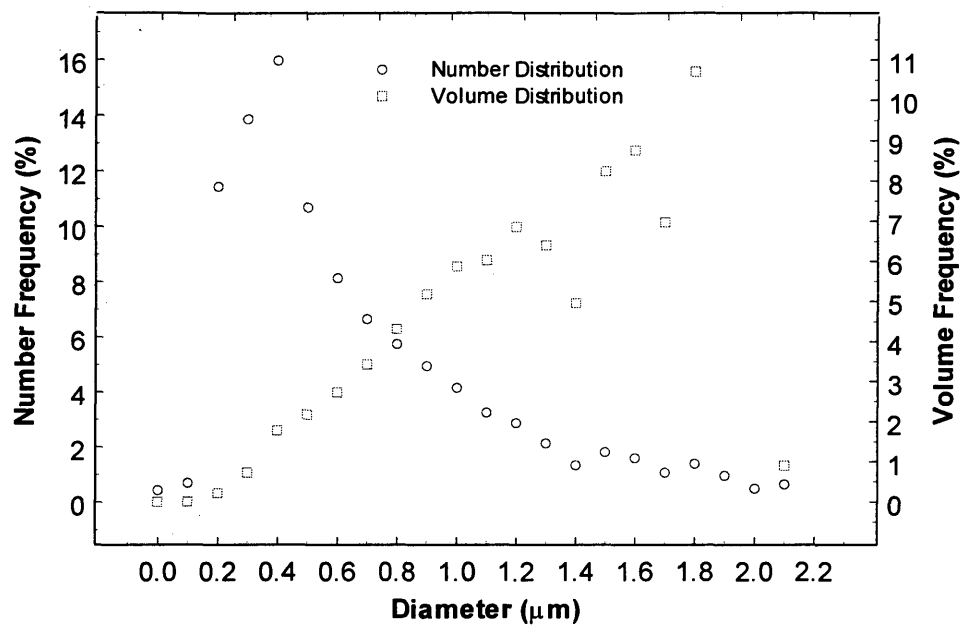


Figure 2.9 - SEM experimental results of the 0.8-2.0 micron Rocky Flats soil fraction, with both the number and volume distributions calculated.

percent of the volume, where a total of 1885 particles are represented. Unlike the two smaller size fractions, this volume distribution more closely matches the size range predicted by the centrifugation calculations.

The particle size distribution representing the fine silt fraction material, 2.0-10 micron (Figure 2.10), illustrates that there are still a large percentage of the particles that are in the smaller size (47.8 percent less than 1.4 micron), but only 0.44 percent of the volume is represented by particles less than 1.4 micron. The volume distribution, however, matches the computed centrifugation size cuts quite well. The linear increase is shown until approximately 6 micron, where the particles then become scattered due to the small number of large particles having large volumes.

2.5.5 FFF

Particle size distributions of the four soil fractions were generated with the FIFFF. Only the two smallest soil samples were analyzed with the SdFFF. Due to the size difference of the particles in the smallest sample to the largest, each sample required a developed method for proper particle elution using polystyrene beads. The conditions necessary for proper separation of the particles are shown in Table 2.3. Online and offline coupling to ICP-MS was also completed to determine whether the FFF runs were mass-based distributions.

2.5.5.1 Normal Mode Elution

The UV-based fractogram and normalized particle size distribution of the less than 0.2 micron fraction of colloidal material for both the SdFFF and FIFFF are shown in Figure 2.11a and 2.11b using normal mode elution. Figure 2.11a illustrates the peak

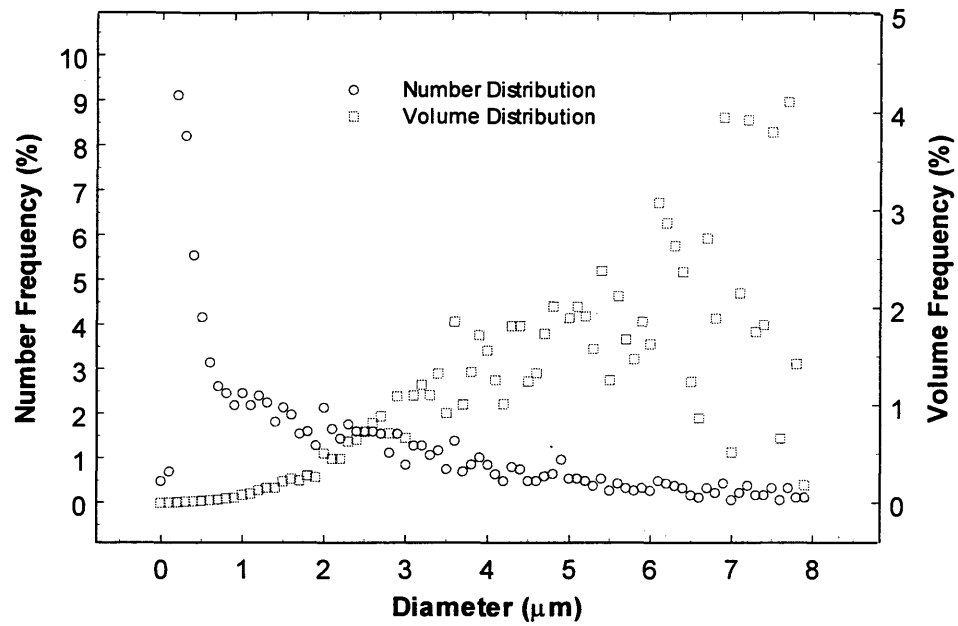


Figure 2.10 - SEM experimental results of the 2.0-10 micron Rocky Flats soil fraction, with both the number and volume distributions calculated.

Table 2.3 - Conditions used for particle separations of Rocky Flat soil fractions. The SdFFF and FIFFF conditions are different for each soil fraction.

<0.2 μm	0.2-0.8 μm	0.8-2.0 μm	2.0-10 μm
SdFFF	SdFFF	FIFFF	FIFFF
t = 54 min	t = 33 min	t = 38 min	t = 30 min
equil = 10.4 min	equil = 20	equil = 6.86 min	equil = 4.36 min
$V^0 = 0.5 \text{ mL/min}$	$V^0 = 1.8 \text{ mL/min}$	$V^0 = 4.0 \text{ mL/min}$	$V^0 = 2.5 \text{ mL/min}$
$\text{RPM}_i = 2440$	$\text{RPM}_i = 765$	$V_c = 0.35 \text{ mL/min}$	$V_{ci} = 0.55 \text{ mL/min}$
$\text{RPM}_f = 105$	$\text{RPM}_f = 53$		$V_{cf} = 0.05 \text{ mL/min}$
$t_1 = 3.3 \text{ min}$	$t_1 = 3 \text{ min}$	t = duration of run equil = equilibration time required	
$t_a = -26.4 \text{ min}$	$t_a = -24 \text{ min}$		
FIFFF	FIFFF	$V^0 = \text{channel flow}$	
t = 100 min	t = 120 min	RPM = revolutions per minute	
equil = 4.0 min	equil = 9.0 min	$V_c = \text{cross-flow}$	
$V^0 = 1.4 \text{ mL/min}$	$V^0 = 2.1 \text{ mL/min}$	t_1 and $t_a = \text{power program field}$	
$V_c = 1.0 \text{ mL/min}$	$V_c = 0.4 \text{ mL/min}$	decay parameters	

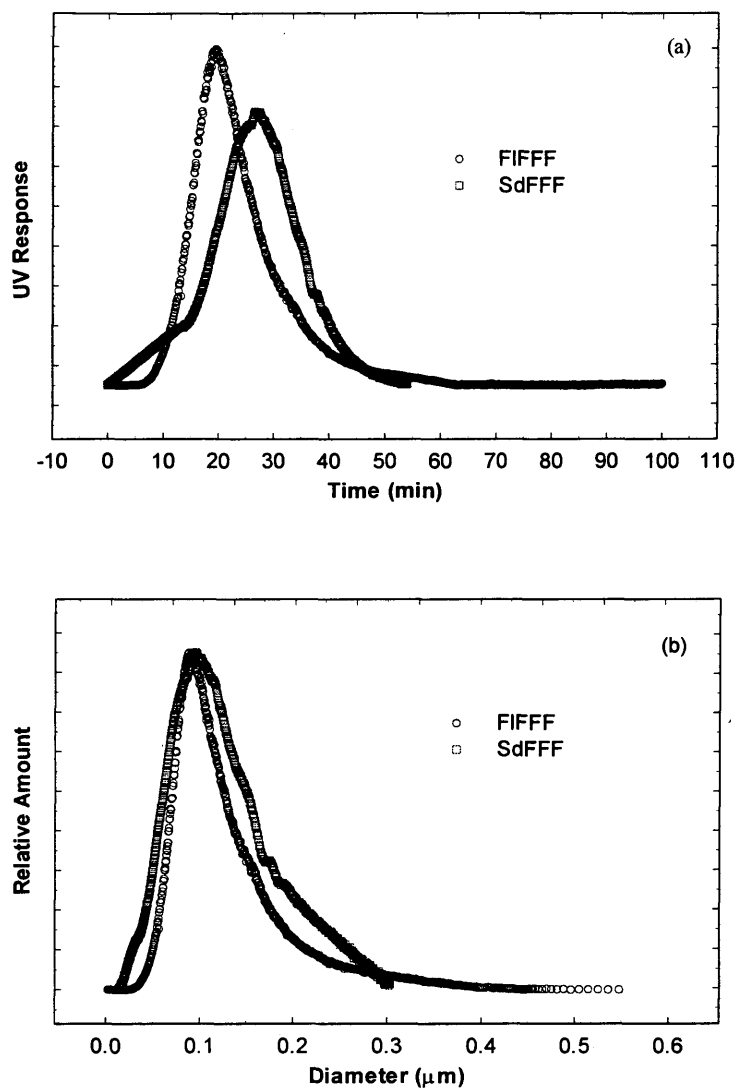


Figure 2.11 (a,b) – Experimental results of the SdFFF and FIFFF of the <0.2 μm Rocky Flats soil fraction. (a) Fractogram illustrates the time versus UV response. (b) Converted fractogram into diameter versus relative amount.

widths are similar in relative time and shape. The time of elution for the two runs is irrelevant in determining size since the field conditions (i.e., channel flow with field generated) determine elution times of the particles. Figure 2.11b illustrates the relative amount of particles for each diameter. The shapes of the curves are very similar for both SdFFF and FIFFF, where the mean sizes of the soil for both FFF methods are estimated to be approximately 0.1 micron in diameter. The peak width of the FIFFF results is somewhat narrower than that for the SdFFF. Comparison of the SdFFF UV data to mass of aluminum in Figure 2.12 demonstrates that a volume distribution is represented for the FFF method. This is reasoned because the Al response closely matches the UV. Aluminum is a major component of soils and should represent the mass of particles eluting from the FFF and therefore it should also follow the UV data if it is a volume distribution. This will be discussed more thoroughly in Chapter 3.

Figure 2.13a illustrates the fractogram of the 0.2-0.8 μm fraction of colloidal material for both the SdFFF and FIFFF. In this figure, the times of elution are very similar to each other, although the UV response is greatly different. The UV response difference is an irrelevant value that is highly dependent upon the sensitivity setting of the UV detector. The SdFFF fractogram still contains its void peak that contains material that is not separated, but it is not shown in Figure 2.13b. In the figure, comparison of the peak is not similar as in the $<0.2 \mu\text{m}$ sample, but is still within 0.1 micron. The SdFFF has determined that the mean size of the sample is approximately 0.152 μm , where the FIFFF is approximately 0.121 μm . Figure 2.14 demonstrates that the elemental distribution of a major element such as aluminum follows the UV data, and thus predicting that the UV-based particle size distributions are representative of a volume distribution. Both the aluminum and the UV follow the same parabolic curve.

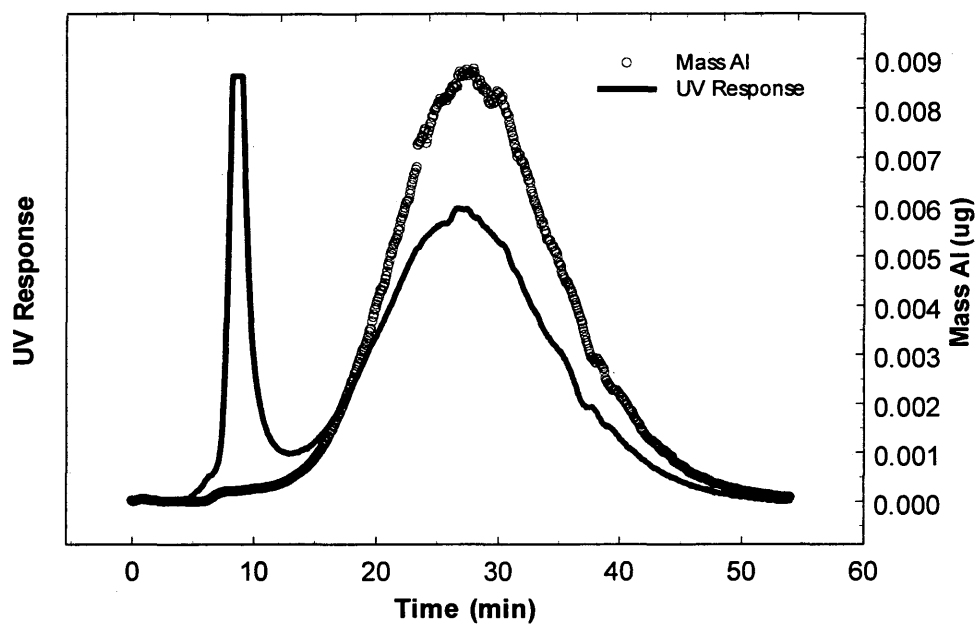


Figure 2.12 – Elemental mass of aluminum compared with the UV response of the SdFFF fractogram for the <0.2 micron soil fraction.

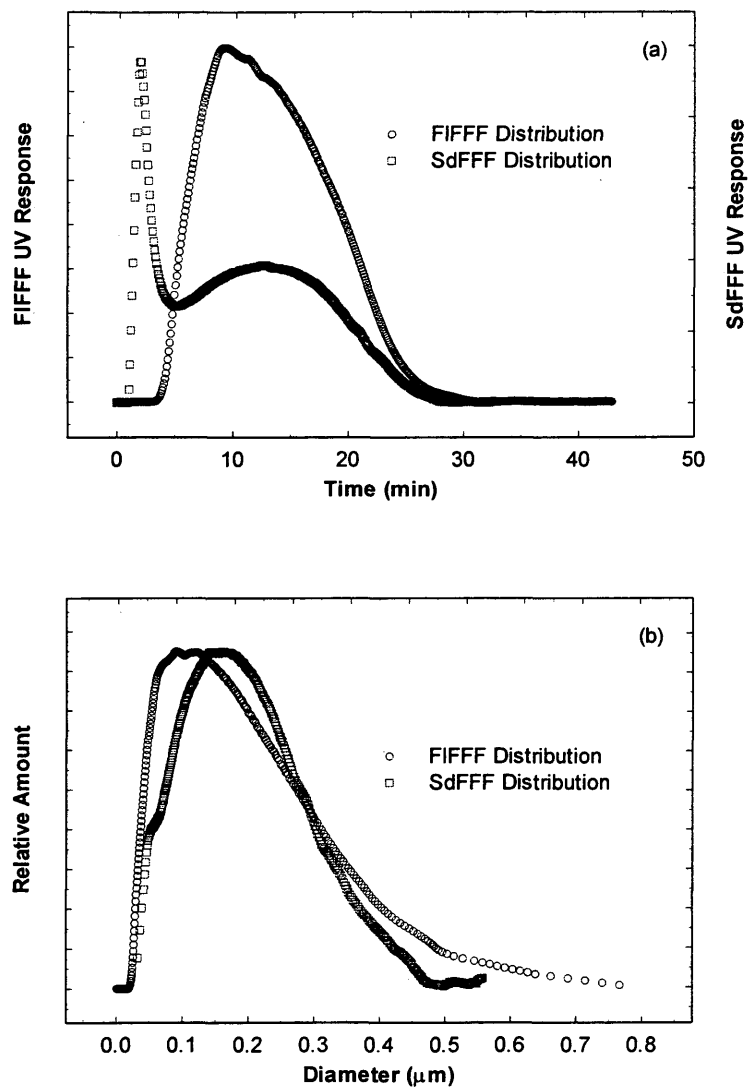


Figure 2.13 (a,b) – Experimental results of the SdFFF and FIFFF of the 0.2-0.8 μm Rocky Flats soil fraction. (a) Fractogram illustrates the time versus UV response. (b) Converted fractogram into diameter versus relative amount.

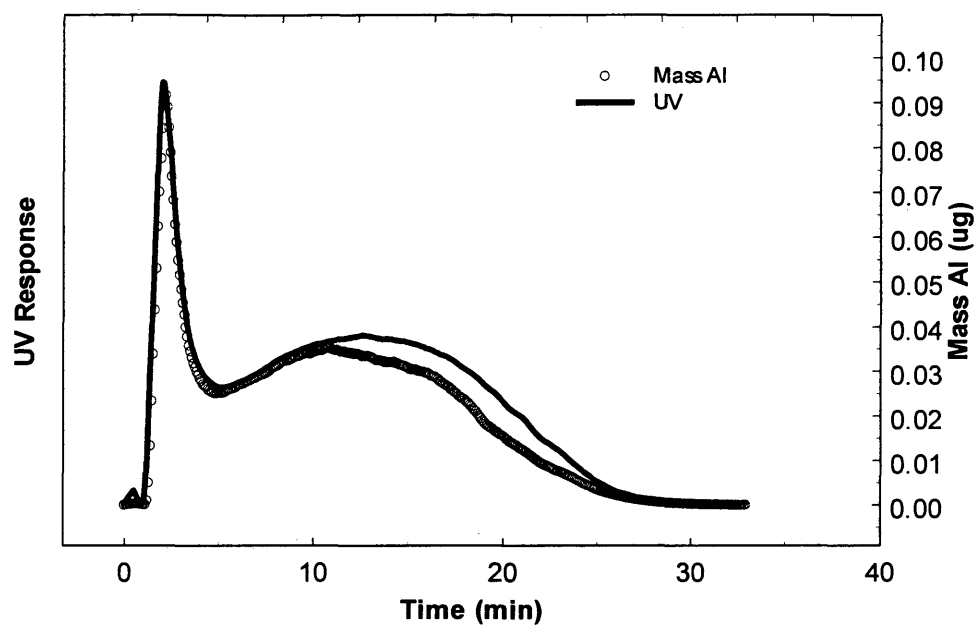


Figure 2.14 – Elemental mass of aluminum compared with the UV response of the SdFFF fractogram for the 0.2-0.8 micron soil fraction.

2.5.5.2 Steric Mode Elution

The two largest samples elute in steric mode, creating a broader separation as the particles get smaller. Since there are not established equations for analyzing the size of the larger particles, one must be developed by comparison with particles of known sizes, such as polystyrene beads. Figure 2.15a compares three established polystyrene bead sizes (2.0, 1.0, and 0.6 μm) and the 0.8-2.0 μm soil fraction. The figure shows that there is a great deal of smaller particles in the size fraction, and that the largest particles are close to 2 μm . Establishing the peak elution time for each bead and creating a plot with a trend-line yields the power equation

$$y = 11.696x^{-1.2503} \quad (2.24)$$

for determining the size of the soils particles, which yields an R^2 of 0.9994. Figure 2.15b is the transformation of the data into particle size using the equation 2.17 and illustrates that most of the particles in the size fraction are smaller than 0.8 μm . Calculation of the mean size yields 0.51 μm . Human errors in calculation of centrifugation time and shape effects are the most probable reasons for the large number of smaller particles.

The largest size fraction is illustrated in Figure 2.16a, which compares the 2-10 μm soil fraction with four polystyrene beads (10, 5, 2, and 1 μm). A bimodal peak represents the soil with the first around 5.5 μm , the second around 1 μm . Establishing the peak elution times of the polystyrene beads and then creating a plot with a trend-line yields the power equation

$$y = 30.193x^{-1.2015} \quad (2.25)$$

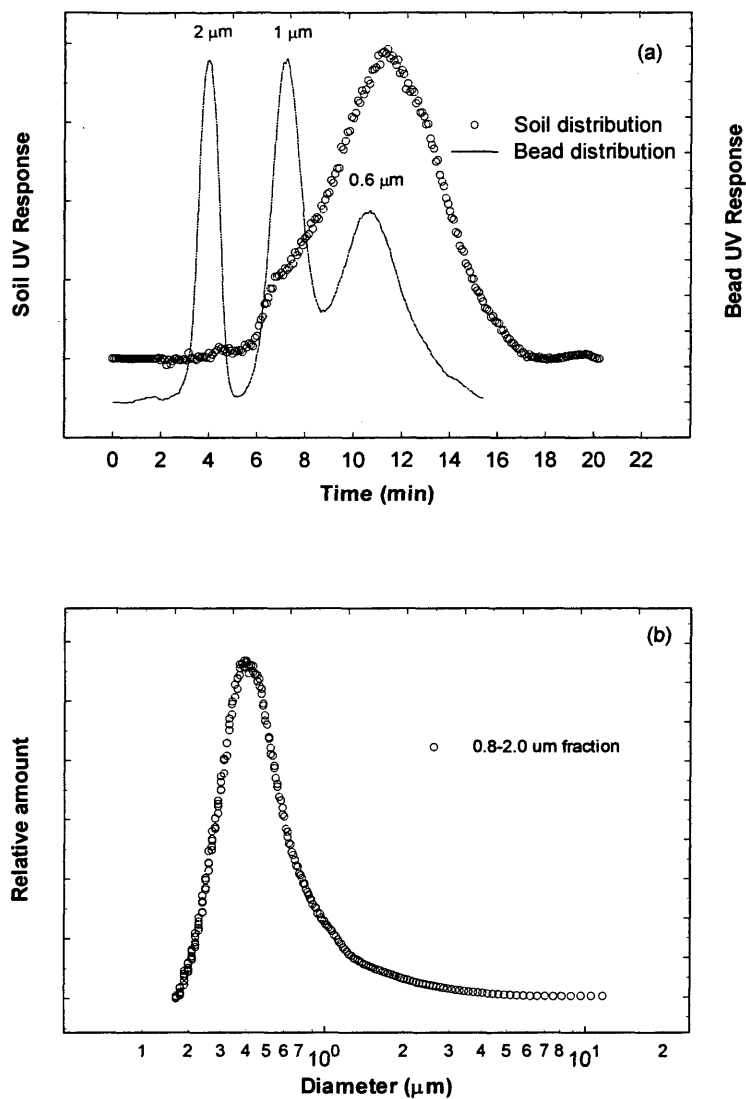


Figure 2.15 (a,b) – Experimental results of the SdFFF and FIFFF of the 0.8-2.0 μm Rocky Flats soil fraction run under steric conditions. (a) Fractogram illustrates the time versus UV response. (b) Converted fractogram into diameter versus relative amount.

for determination of the size of the soil particles, which yields an R^2 of 0.9886.

Transformation of the data using equation 2.17 yields a distribution with a mean size of 1.08 μm . When plotted on a logarithmic scale (Figure 2.16b), a broad peak of larger particles (approximating between 2 and 10 μm) is present, as well as a peak representing particles as small as 0.6 μm .

2.6 Conclusion

Natural soil colloids present a problem of analysis for all techniques of particle sizing. Theory is generally centered on spherical particles of similar physical characteristics such as refractivity, mass, and composition. Natural soil colloids are typically not perfect spheres, so measurements of the particles are skewed either higher or lower than their actual size. Table 2.4 summarizes the results from the particle sizing techniques. Centrifugation, using Stokes Law of Settling, provides crude size fractions. In smaller fractions, there are few larger particles. These few larger particles, though, skew volume distributions to larger sizes. The larger sized fractions contain large numbers of smaller particles, which skew number distributions towards a smaller mean size.

PCS has been shown to be unusable for environmental soil colloids. In the course of experimentation, a mean size was calculated approximately 30 times, but failed to give a distribution of particles. Therefore the instrument calculated results favoring the large number of smaller particles instead of a mass based mean size. The results are located in Table 2.4.

Using SPOS to size analyze soil colloids works very effectively and efficiently. The particle size distributions elaborately display the size and volume information, with mean sizes best represented with the volume distribution as seen in Table 2.4. The ability to only count and not conduct other analyses on the colloids is a downfall of using SPOS, as well as the limitation of 0.5 μm sized particles to be analyzed.

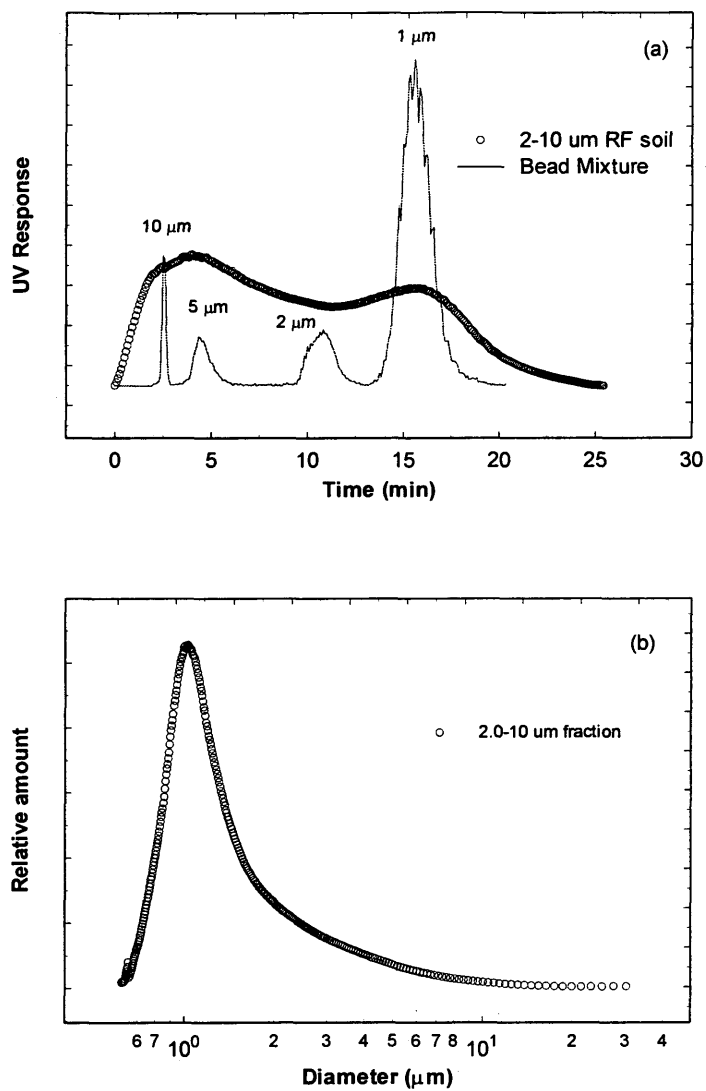


Figure 2.16(a,b) – Experimental results of the SdFFF and FIFFF of the 2.0-10 μm Rocky Flats soil fraction run under steric mode elution. (a) Fractogram illustrates the time versus UV response. (b) Converted fractogram into diameter versus relative amount.

Table 2.4 - Mean size distribution of the Rocky Flats colloids using the various particle-sizing methods. There are two types of distributions shown: number and volume. The values are representative of the mean size in microns.

Size Class	PCS	FIFFF	SdFFF	SPOS		SEM	
	Number	Volume	Volume	Number	Volume	Number	Volume
<0.2 μm	0.16	0.107	0.100	-	-	0.26	2.22
0.2-0.8 μm	0.28	0.121	0.152	-	-	0.28	1.72
0.8-2.0 μm	0.35	0.51	-	0.61	1.12	0.49	1.78
2.0-10.0 μm	0.45	1.08	-	0.54	5.96	1.43	5.55

The particle size distributions created from the SEM data was very random, as seen in Table 2.4. All the size fractions have a large percentage of smaller particles, as seen in Figure 2.17. There is very little difference between the two smallest fractions, with the exception that the less than 0.2 fraction seems to have an unusual number of larger particles. They both peak around 0.2 μm and baseline out at approximately 0.8 μm , with the 0.2-0.8 μm fraction having a higher percentage of particles in this range. The larger fractions have a reduced amount of the smaller particles and have a higher baseline percentage of larger particles, which constitutes higher volume distributions. When analyzing the volume distribution, the general progression is for the larger size fractions to have more volume in the higher numbers, with the exception of the smallest fraction. This phenomenon could be the result of contamination, or poor sampling.

FIFFF and SdFFF have shown potential for particle sizing and can couple chemical analysis such as ICP-MS to achieve chemical composition versus size. Size effects still limit the effectiveness of the FFF, just like the other techniques. The mean size of each size fraction is listed in Table 2.4. The FFF represents a volume distribution, which is proven with the distribution following the major chemical component response. Figure 2.18 illustrates the separation of the particles for all the size classes. As seen, the general progression shows that the larger size fractions have a peak size later than their smaller counterparts. The mean sizes of the particles also get bigger for the larger size fractions, proving that the technique is feasible for size analyzing natural soil colloids.

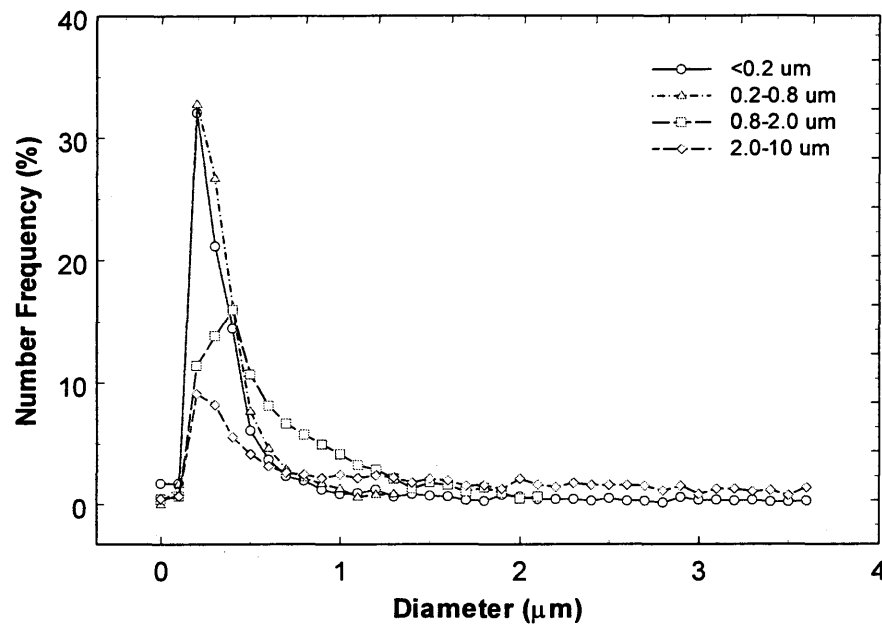


Figure 2.17 – The four soil fractions examined with the SEM are compared. Note that the margins have been cut for better resolution.

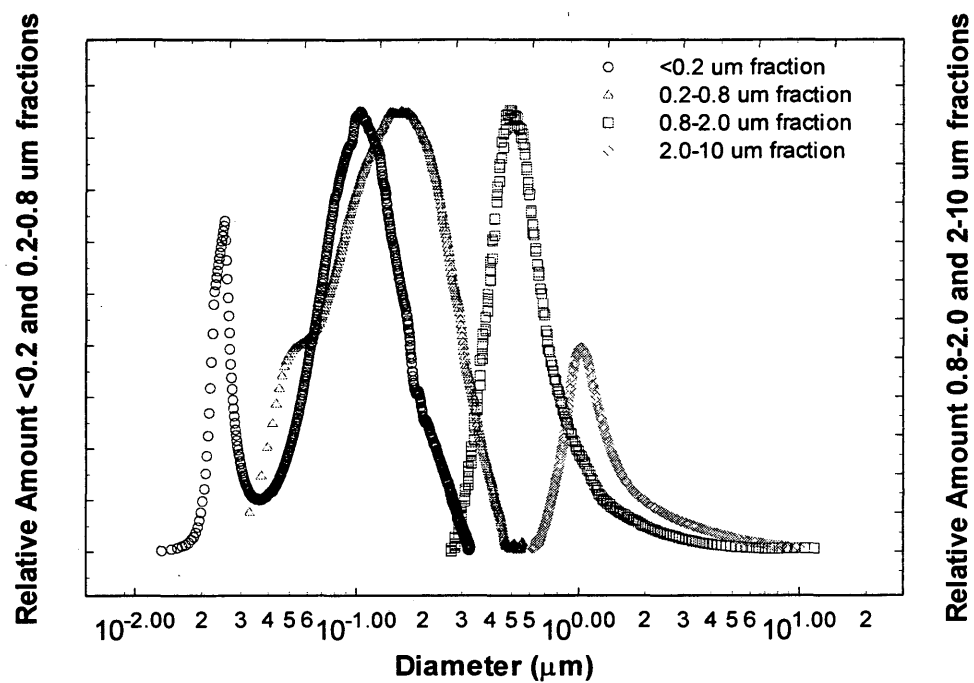


Figure 2.18 – The four soil fractions run through the FIFFF are examined. The conditions for each run have been previously explained.

CHAPTER 3

CHEMICAL ANALYSIS VERSUS SIZE

3.1 Introduction

Environmental soil colloids are highly variable in size, shape, and chemical composition. One of the ways that colloids are formed is through mechanical and chemical weathering of parent material; thus the composition varies by geographical location. Other colloidal particles are generated through either chemical or biochemical production are biological debris or from resuspension of sediments (Buffle and Leppard, 1995). Generally, each particle is composed of major and minor elements such as silica (Si)², aluminum (Al), and iron (Fe), but concentrations of each are variable. Elements are also found in trace concentrations in soils, which can have even greater variability. The trace elements can typically be found on the surface of the colloidal particles, due to the increase in specific surface area with decreasing size.

The size of the particles can be relevant when surface coatings are present, which can alter the surface charge of the particle. This can help influence the transport of materials such as heavy metals, radioactive materials, biological entities (i.e. viruses, bacteria, etc) and organics (Ranville et al., 1999; Kaplan et al., 1993). This directly applies to the surface charge exhibited by the particles. The electrostatic charge of the particle, as well as the charge of the media in which the particle has contact, can determine the potential retention of colloids through adsorption or desorption in soils and groundwater (Elimelech et al., 2000). The composition of the media, or soils, is highly variable by location. In many areas, soils have a high percentage of quartz as a major constituent.

² Silica is a major element that typically has concentration of 2.5 to 3 times that of minor elements such as Al and Fe.

Other minerals that can be found include (but are not limited to), feldspar, biotite, iron hydroxide clays, calcite, zeolite, and organic matter (Degueldre et al., 2000).

Colloidal particle concentrations and types of colloids present are highly dependent upon environmental conditions such as pH, redox potential, organics, and ionic strength of ions such as Mg, Na, Ca, and K (Degueldre et al., 2000). Colloids stability is affected by these environmental parameters. A high ionic strength will have a tendency to retain particles to media surfaces. A low pH will tend to dissolve colloidal particles.

Incorporation of chemical analysis instruments such as inductively coupled plasma-mass spectrometry (ICP-MS) and graphite furnace atomic adsorption (GFAAS) are promising applications for defining chemical compositions of particles and sizes of colloidal particles when coupled with a suitable separation technique such as FFF. The potential of coupling FFF with either ICP-MS or GFAAS seems promising to study the factors influencing transport of colloids and potential contaminants adsorbed to the surface of the particles. Not only can it determine the existence of surface coatings, but also a change in the mineralogy of the colloidal particles. Certain mineralogical phases (i.e., kaolinite, vermiculite, illite, etc.) may exist more dominantly in certain size ranges than in others.

3.2 Analytical Chemistry Techniques Utilized to Determine Elemental Composition

In the course of experimentation, ICP-MS and GFAAS were utilized to analyze the colloidal particles by coupling of the instruments to a FFF sub-technique. This was completed through both online³ and offline⁴ coupling. Both coupling techniques are discussed below.

³ Online coupling has a direct connection to the FFF to give real time analysis of chemical composition versus size.

⁴ Offline coupling entails collecting timed fractions with a fraction collector and conducting the analysis

3.2.1 Inductively Coupled Plasma-Mass Spectrometry (ICP-MS)

The ICP-MS instrument used was the ELAN 6100 ICP-MS, developed by Perkin-Elmer. The ICP-MS method provides a multiple element trace analysis of soils. The standard design centers around a high temperature (7000-10,000 degrees Celsius) plasma generated from argon gas flowing through three concentric quartz tubes. Surrounding the top of the largest tube is a water-cooled induction coil powered by a radio-frequency generator. Argon is then ionized from a spark from a Tesla coil⁵. Freed ions and electrons then interact with the magnetic field generated by the induction coil. The high temperature of the plasma is generated through the resistance of the ions and electrons to their circular orbits produced by the magnetic field (Skoog and Leary, 1992). The ICP-MS “is operated at atmospheric pressure with a quadrupole mass analyzer, which requires a moderately high vacuum (10^{-6} - 10^{-5} mbar) and a stable temperature close to room temperature” (Tadjiki, 1999). The sample is most commonly injected into the ICP-MS using a nebulizer, which creates finely divided droplets and carries them into the plasma, where they are atomized. There are many variations in nebulizers, which include: ultrasonic nebulizer, electrothermal vaporization, and direct injection nebulizer. These methods are more thoroughly detailed in Skoog and Leary (1992).

The ICP-MS has distinct advantages over other analytical techniques. The most important advantage is the ability of ICP-MS to conduct multi-element analysis with a high sensitivity, usually with limits of one part per trillion or less depending on the instrument and element measured (Tadjiki, 1999). A high resolution ICP-MS can distinguish isotopes of an element and between elements of similar masses. ICP-MS is also desirable due its suitability for online coupling to size separation techniques such as FFF (Hassellöv et al., 1999; Ranville et al., 1999). This produces a high-resolution

⁵ Tesla coils are air-core, resonant transformers that work at high frequencies and can generate tremendous voltages.

chemical composition analysis to be compared with the size of the particle, which then can be applied to such fields as contaminant transport potential.

ICP-MS, while accurately measuring concentrations for most elements, can have a difficult time measuring some elements, namely Ca and K. The interference originates from the argon gas having a mass of 40, which is similar to Ca and K. Other elements with larger detection limits include Fe, Si, P, and S (Tadjiki, 1999).

3.2.2 Graphite Furnace Atomic Absorption Spectrometer (GFAAS)

The GFAAS instrument used was the AAnalyst 800 Spectrometer, developed by Perkin-Elmer, which is an automated interchangeable flame/graphite furnace AAS. The GFAAS instrument uses argon gas to atomize the particles into gaseous atoms, which are then measured spectroscopically. This is accomplished with a graphite tube that is heated with a high current and low voltage power supply. The graphite tube has an inner diameter of 3 to 6 mm and a length of 20 to 40 mm, which is held in place by water-cooled electrodes, which help control the temperature. The temperature of the tube can be controlled with little deviation up to 2700 degrees Celsius. The sample is injected into an inert atmosphere⁶ through the dosing hole in the center of the furnace length, where it comes in contact with the source beam, which atomizes the sample and forms an atomic cloud. The source beam passes through the center of the tube to the detection system, which utilizes a quartz window to prevent the intrusion of oxygen into the furnace. The atomic cloud has a fairly long residence time due to diffusion necessary for mass transport (Butcher and Sneddon, 1998; Welz and Sperling, 1999).

With the AAnalyst 800 Spectrometer model of GFASS, it was possible to only analyze one element at a time. Newer models enable multi-element analysis, but the

⁶ The inert gas used is typically argon because of its unreactive nature. Nitrogen is not as favorable due to its reactive nature with several elements such as Al.

samples must still be collected in a fraction collector for analysis, which can be time consuming. Analysis of each sample is time consuming as well. The graphite tube must be heated and cooled to the programmed temperature, which took approximately seven minutes per sample. Even with all the disadvantages of using GFAAS, it has a high resolution necessary for trace element analysis.

3.3 Results and Discussion

Chemical composition versus size of natural soil colloids from Rocky Flats was desired. Online coupling was conducted with the SdFFF and ICP-MS for the less than 0.2 micron and 0.2-0.8 micron samples. The conditions for the FFF used to size fractionate the samples can be seen in Table 3.1. Analysis of the chemical data was aimed at silica (Si), aluminum (Al), iron (Fe), magnesium (Mg), potassium (K), manganese (Mn), and uranium (U). These elements were selected to measure examples of primary (Si), secondary (Fe, Al, Mg, K), and trace (Mn, U) elements in the soil. Proof of changes in surface coatings or mineralogy changes was sought. Other elements were measured, but not analyzed. Offline coupling was conducted between the GFAAS and FIFFF with a hematite sample, with an analysis of the Fe content. The offline coupling was conducted to determine feasibility of analysis with the GFAAS. The results are described below.

3.3.1 Offline Coupling of FIFFF to GFAAS

A suspension of hematite created by Dr. Richard Murphy with a size of approximately 60 to 90 nanometers in size was used in this experiment, which was

Table 3.1 - SdFFF conditions used for size analysis of the soil fractions.

<0.2 μm	0.2-0.8 μm	Parameters
SdFFF	SdFFF	t = duration of run
t = 54 min	t = 33 min	equil = equilibration time required
equil = 10.4 min	equil = 20	V^0 = channel flow
$V^0 = 0.5 \text{ mL/min}$	$V^0 = 1.8 \text{ mL/min}$	RPM = revolutions per minute
$\text{RPM}_i = 2440$	$\text{RPM}_i = 765$	V_c = cross-flow
$\text{RPM}_f = 105$	$\text{RPM}_f = 53$	t_1 and t_a = power program field
$t_1 = 3.3 \text{ min}$	$t_1 = 3 \text{ min}$	decay parameters
$t_a = -26.4 \text{ min}$	$t_a = -24 \text{ min}$	

prepared in a solution of 0.01% sodium azide and 0.01% FL-70 surfactant. The sample was injected into an FIFFF channel with a V^0 of 1.529 mL/min, V_c of 1.0 mL/min, and an equilibration time of 4.0 minutes. Fractions of the run were collected after the UV detector every minute for the first 30 minutes, and every 2.5 minutes the next 60 minutes. After collection from the FFF, the fractions were run through the GFAAS to determine the concentration of Fe in the hematite. Since hematite is chemically uniform in Fe, the UV response and the concentration of Fe in the fractions should follow similar content patterns if the UV detector is sensitive to mass. Figure 3.1a demonstrates that the Fe follows the UV, with both having bimodal peaks, meaning that the hematite is not homogeneous in size, but rather there are at least two main sizes of hematite aggregates. The UV response is directly influenced by the change in Fe concentration, which is represented in the Fe/UV ratio. In Figure 3.1b, the UV versus Fe concentration yields a linear result. With an R^2 of 0.87, the Fe concentration tends to increase as the UV increases.

This experiment was conducted to determine the feasibility of coupling GFAAS and FFF techniques, which was shown to have potential, especially with chemically homogeneous samples. When trying to analyze a natural soil colloid though, it is not

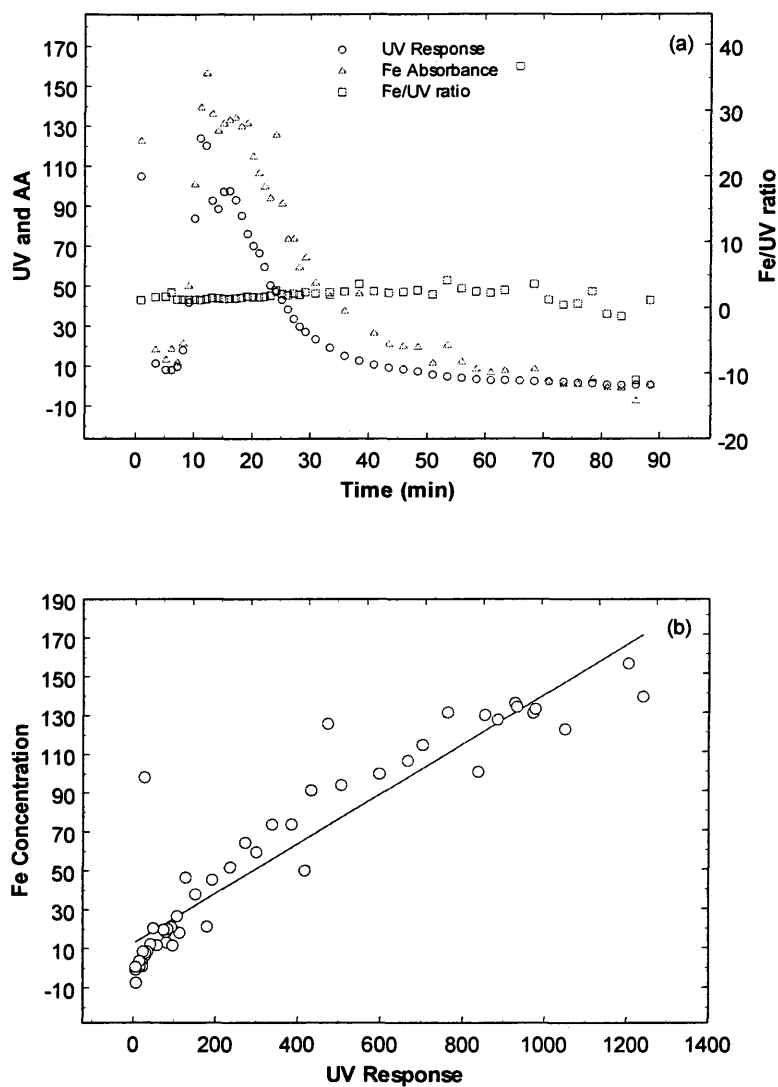


Figure 3.1(a,b) – Offline coupling of GFAAS with FIFFF yielding (a) Fe concentration and UV, respectively, with the Fe/UV ratio plotted. (b) The ratio plotted on separate axis show a linear relation between the two.

feasible to use GFAAS if analyzing for a large number of elements due to the ability to only measure one element at a time. The advantage of GFAAS is in its high sensitivity, which can make this appealing when measuring trace elements.

3.3.2 Online Coupling of SdFFF to ICP-MS

Online coupling of ICP-MS to SdFFF was completed to analyze the two smallest fractions of Rocky Flats soils. Particle size distributions were generated from the SdFFF. The mass of each element eluting at each time period was calculated from the ICP-MS data and presented in conjunction with the UV data. Due to the small size of the particles, it is believed that the SdFFF was able to elute the particles in normal mode.

3.3.2.1 Analysis of the <0.2 Micron Rocky Flats Soil Fraction

The smallest size fraction of Rocky Flats soils was conducted under the conditions listed in Table 3.1 through normal mode elution. Figure 3.2a represents the mass of the Si, as well as the UV from the SdFFF, over the duration of a run. The Si and UV data both peak at the same time, which is approximately 28 minutes. The UV shows a large void volume, which can be attributed to particles that are not retained near the accumulation wall, such as dissolved species. The mass of silica in the void volume is shown to be only 3.16 percent of the mass of Si measured through the entire run indicating no significant dissolved Si was present. Using a typical value for the retention parameter, R , of 0.5, any particles found before 2.0 void volumes⁶ cannot accurately be measured. So any particles that elute before 16.8 minutes cannot be analyzed for size. A line on the graph illustrates the lower effective particle-sizing limit. In Figure 3.2b, the

⁶ The retention parameter, R , is inversely proportional to the number of void volumes.

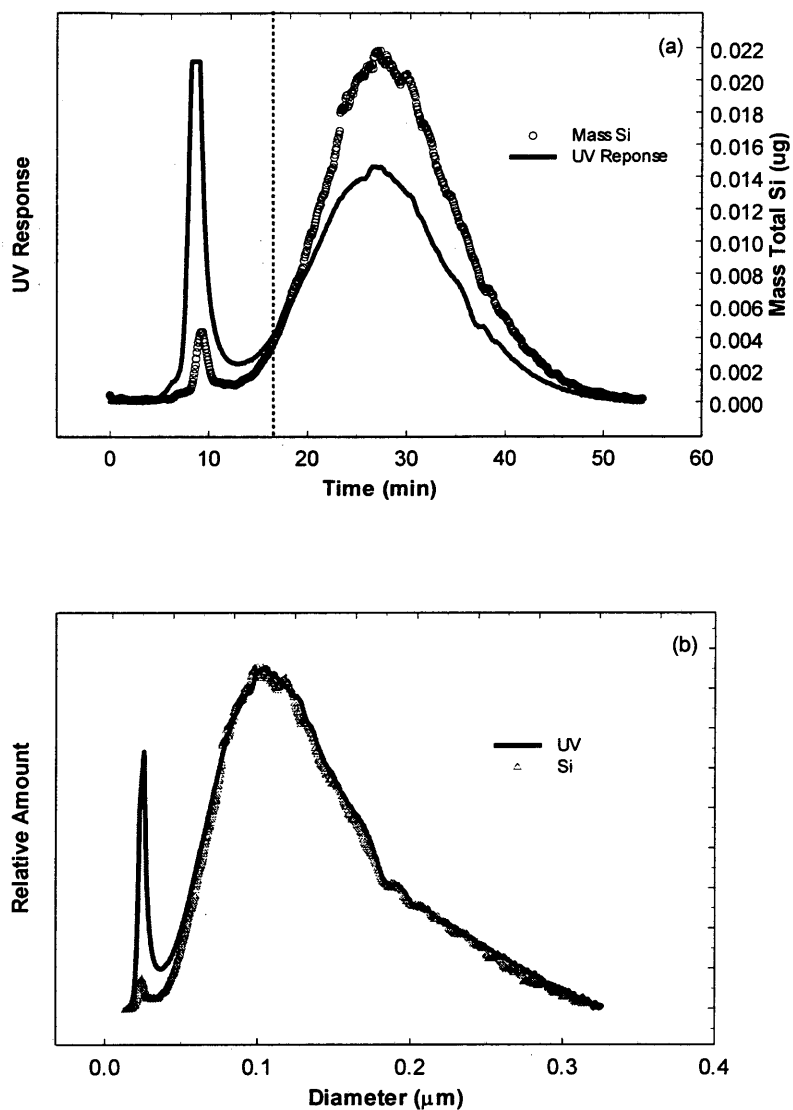


Figure 3.2(a,b) – Normal mode elution SdFFF of the <0.2 μm fraction of Rocky Flats soils coupled with ICP-MS. (a) Fractogram representation of time versus mass Si and UV from FFF. (b) Converted fractogram into relative amount Si and UV versus diameter.

relative amounts of the UV and Si overlap, with the exception of the void volume. This shows that as the particles are mostly composed of Si, but are not in the dissolved phase where it would elute with the void volume. The result also suggests that UV response is proportional to particle mass. The Si isotopes represent approximately 55 percent of the mass of the sampled elements, thus Si can be considered to be the primary component of the colloidal material, consistent with the mineralogy of the soil. The percentage mass was calculated by the summation of the element, divided by the summation of all the sampled elements.

When analyzing secondary elements (e.g. Fe, Al) in a natural soil, the UV and mass data should be similar in shape if the element is dispersed throughout the entire colloidal particle. If a particular element has an elemental ratio that is higher with particles of smaller diameter, the element is likely to be present in surface coatings. Surface coatings will be concentrated with smaller particles due to their substantially larger surface area per unit mass than that of larger particles. When analyzing the Fe and Al masses in Figure 3.3a, the peaks are similar in shape, with peaks close to 28 minutes. Only the UV response from the SdFFF has a large void peak. A large void peak suggests that elemental mass is found in the dissolved phase or very small particles. The elements are shown to follow the UV, demonstrating that the minor elements in this soil are a component of the soil and not represented as a surface coating. Analysis of the Fe/Si and Al/Si ratios in Figure 3.3b yield potentially small amounts of surface coatings with the smaller particles (which elute first). At the tail end of the curve, the Fe and Al increase as well, supporting either an error in analysis of the data or a change in the mineralogy of the colloidal material. Figure 3.3c compares the size distributions of the elements with the relative amount of each element. The relative amount of each element generally follows the UV, indicating the elemental concentrations are evenly dispersed throughout the colloidal particles. If the peak of the element had been different than the UV, it would have indicated a probable mineralogy change or some form of surface coatings. The Fe and Al in the particles represent 8.3 and 22.0 percent of the mass of measured

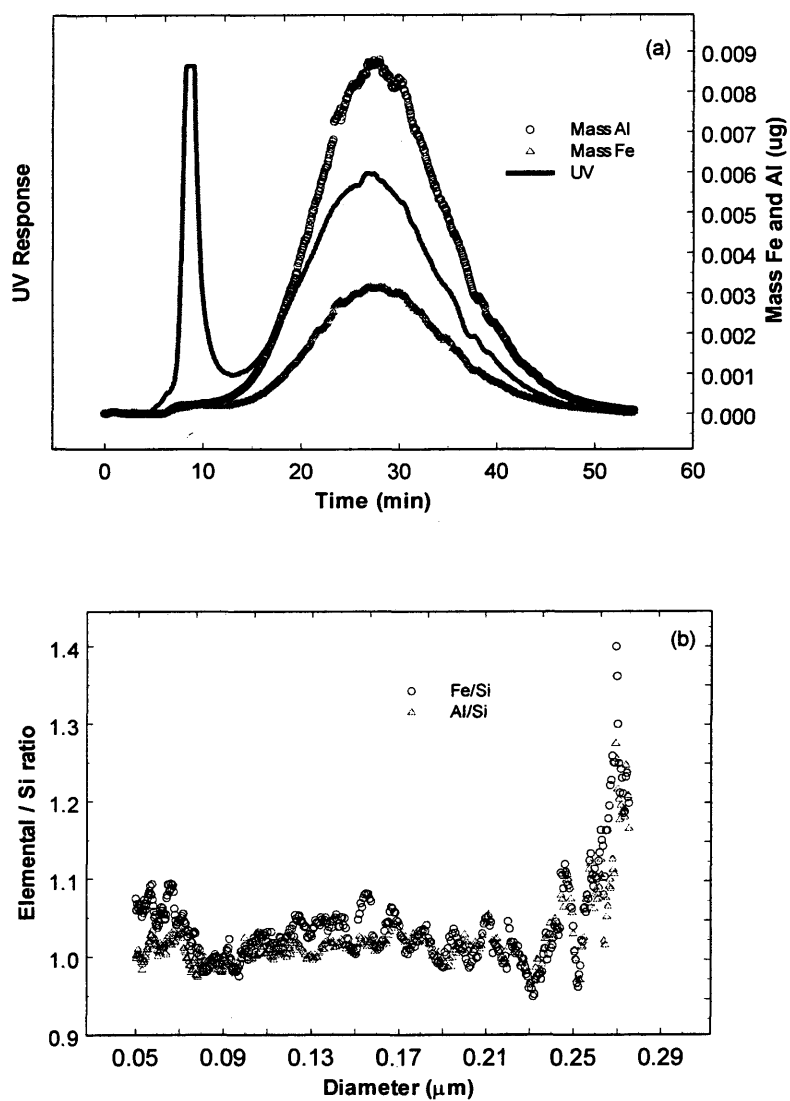


Figure 3.3(a,b) - Normal mode elution SdFFF of the $<0.2 \mu\text{m}$ fraction of Rocky Flats soils coupled with ICP-MS. (a) Fractogram representation of time versus mass Fe, Al, and UV from FFF. (b) Size representation of the Fe/Si and Al/Si ratios.

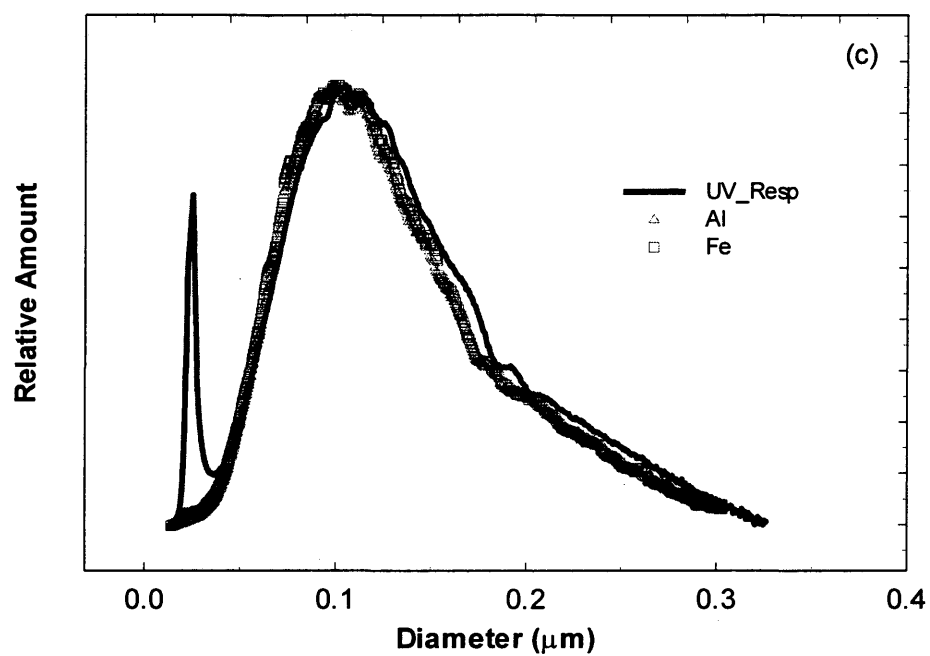


Figure 3.3c - Normal mode elution SdFFF of the $<0.2 \mu\text{m}$ fraction of Rocky Flats soils coupled with ICP-MS. Converted fractogram into relative amount Fe, Al, and UV versus diameter

elements, respectively, in the colloidal particles over the course of the run, making them secondary components of the particles.

Elemental ratios were also calculated for K and Mg, which represent other secondary components of the soils. In Figure 3.4, the Mg/Si ratio yields potentially small amounts of surface coatings due to the small slope of the smaller particles (approximately 10%). The tail end of the ratio that is representative of larger particles is highly scattered, and therefore does not probably have any significance. In the K/Si ratio, there is a large drop in the ratio for the smaller particles (approximately 60 percent). Because it is unlikely to be adsorbed on the surface of inorganic particles, it is indicative of a type of organic coating.

Considering the high resolution of the ICP-MS, trace element analysis is a feasible feature to utilize. Elements such as Mn and U, which are found in natural soil colloids in trace concentrations, can be measured as long as the concentration is within the ICP-MS detection limitations. Figure 3.5a represents the timed elution of the particles from the channel and the elemental masses associated with the UV. The Mn, as seen in the figure, has most of its mass in the void volume (approximately 62 percent). With most of the mass in the void volume, the Mn is either in dissolved form or has formed very small particles that elute with the rest of the void volume. The high amount of Mn found in the void volume could be the result of dissolution from the surface of the particles during sample preparation and storage. The Mn could also be present in colloids that are too small to be measured with the method, but large enough to be retained by the 10,000 Dalton filter. An alternative explanation is that Mn is associated with colloid organic matter. Analysis of the Mn/Si ratio (Figure 3.5b) shows the Mn coatings present in the smaller particles. Although the ratio is low, there is a dramatic increase in the amount of Mn present with the smaller particles, even with the void peak excluded. The U/Si ratio in Figure 3.5b shows a little change in smaller particles, demonstrating a potential for surface coatings, but is generally constant. The tail end of the run shows highly scattered results that make it difficult to determine if a mineralogy change is occurring.

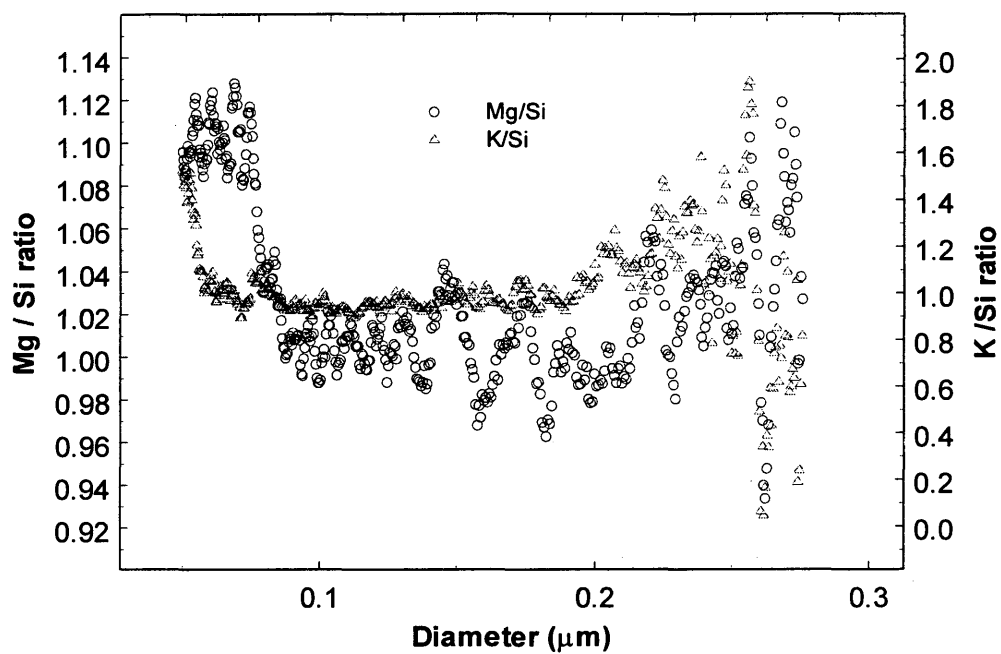


Figure 3.4 - Normal mode elution SdFFF of the $<0.2 \mu\text{m}$ fraction of Rocky Flats soils coupled with ICP-MS. The K/Si and Mg/Si ratios are plotted versus diameter.

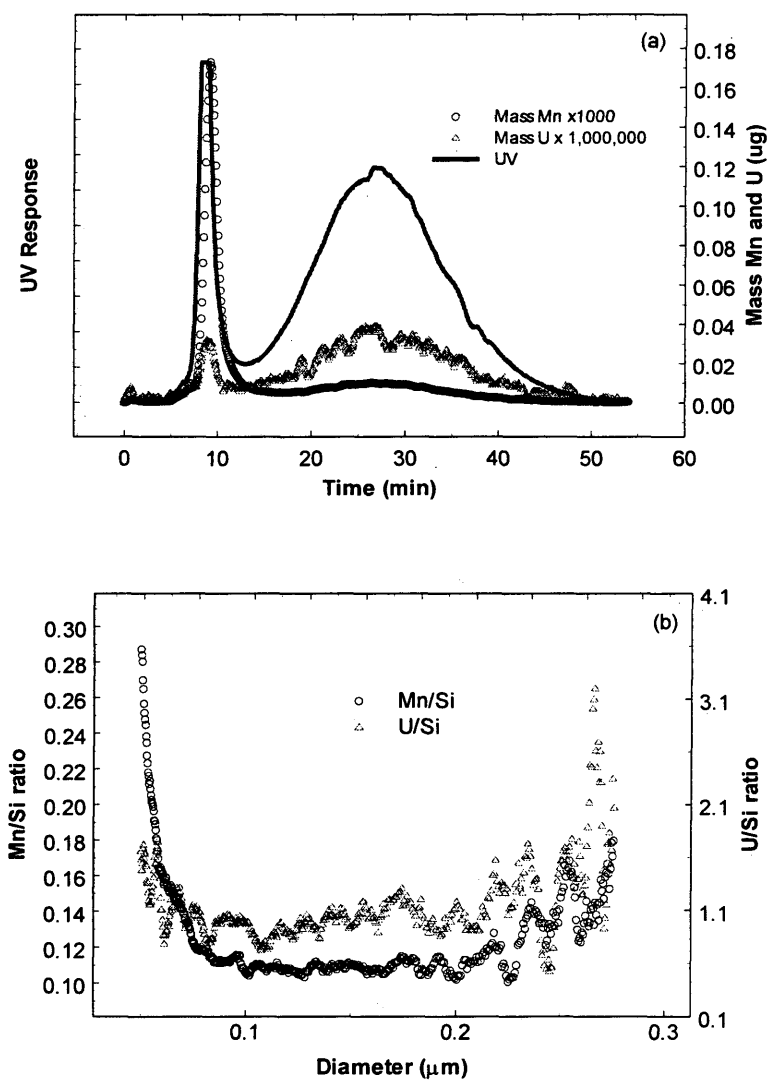


Figure 3.5 (a,b) - Normal mode elution SdFFF of the $<0.2 \mu\text{m}$ fraction of Rocky Flats soils coupled with ICP-MS. (a) Fractogram representation of time versus mass Mn, U, and UV from FFF. (b) Size representation of the Mn/Si and U/Si ratios illustrating potential coatings and mineralogy change.

Figure 3.5c shows the U has a small void volume (approximately 14 percent) and is similar in shape to the UV response for the smaller particles, while containing higher amounts in the larger sized particles, which could illustrate a slight mineralogy change. The U peaks at approximately 0.1 micron. The Mn, however, is biased towards the void volume; the general shape of the curve after the void peak is also similar to the UV, with the main peak occurring at approximately 0.1 micron. The U and Mn represent 0.00012 and 0.087 percent of the mass in the colloidal particles, respectively.

3.3.2.2 Analysis of the 0.2-0.8 Micron Rocky Flats Soil Fraction

The conditions that were established to best separate the 0.2-0.8 micron size fraction of Rocky Flats soils using the SdFFF for normal mode elution can be found in Table 3.1. The duration of the run lasted approximately 33 minutes to size fractionate the soils. Figure 3.6a represents the mass of the Si from the ICP-MS and the UV response from the SdFFF. The figure shows that the Si is different from the UV due to an early decrease in the mass of Si. The larger particles must have higher concentrations of other some elements. Both the UV and the mass Si have large void volumes, which can be either dissolved species or smaller colloidal particles that come out with the void volume. The mass of silica in the void volume represents approximately 20.8 percent of the Si mass. Using a typical value for R of 0.5, any particles found before 2.0 void volumes cannot accurately be measured. So any particles eluted before 4.7 minutes cannot be accurately represented. A line on the graph demonstrates the cutoff of the effective particle sizing. In Figure 3.6b, the relative amount of both the UV and Si are similar in shape, but the Si has a very slightly displaced result. The Si is represented in higher proportions of the smaller than larger sized particles. The Si represents approximately 69.3 percent of the mass of the analyzed elements, making it the major component of the colloidal material.

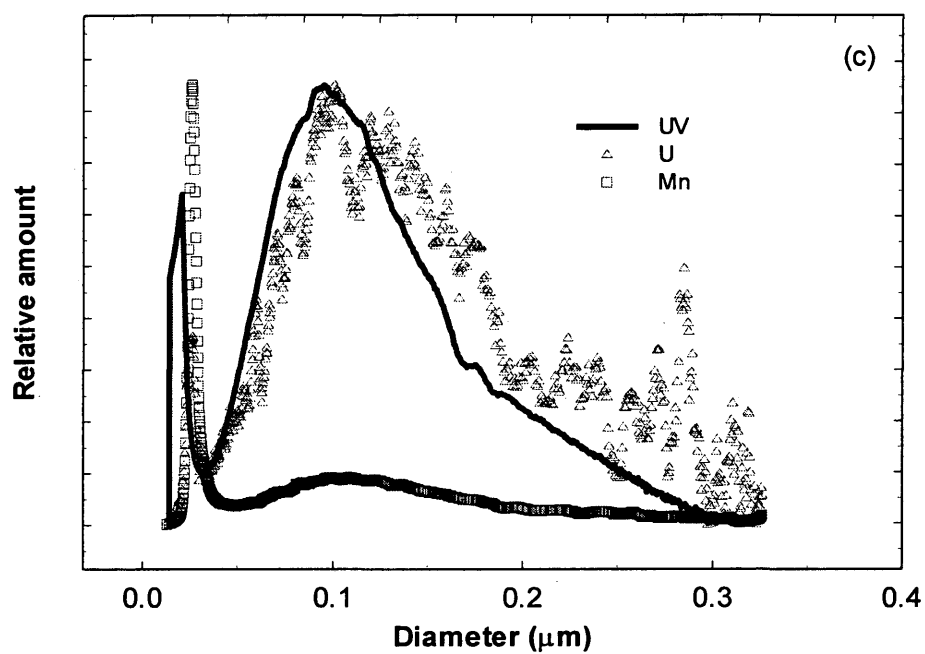


Figure 3.5c – Normal mode elution SdFFF of the $<0.2 \mu\text{m}$ fraction of Rocky Flats soils coupled with ICP-MS. Converted fractogram into relative amount of Mn, U, and UV versus diameter.

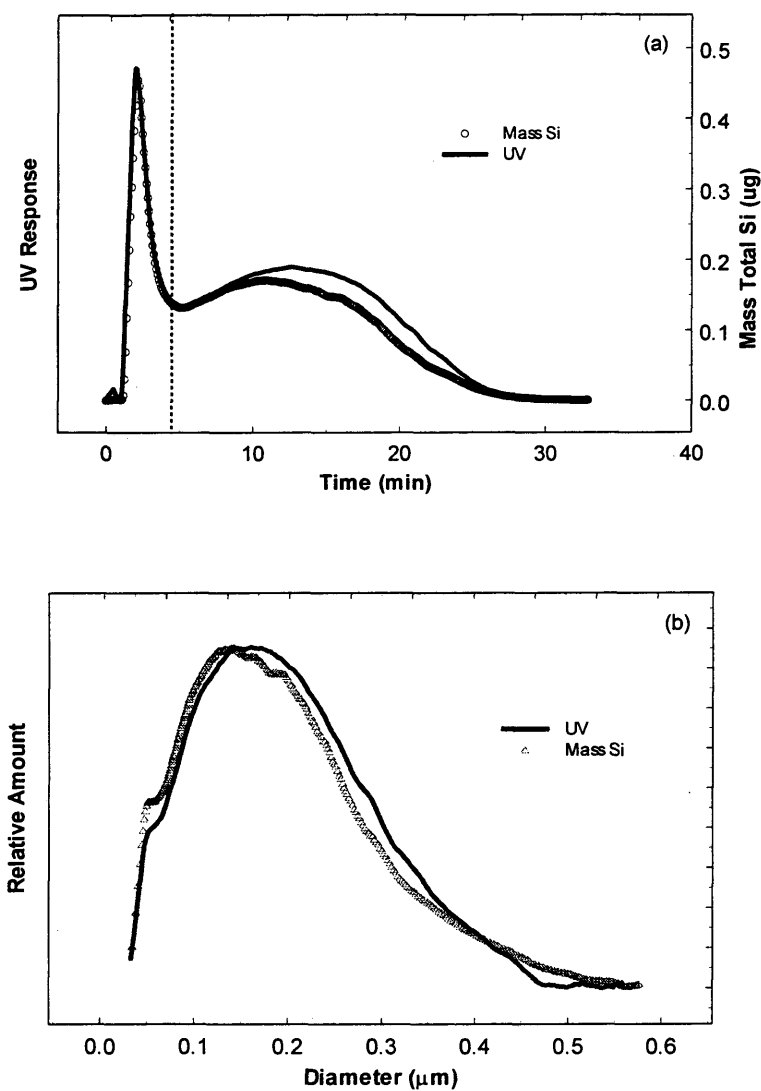


Figure 3.6 (a,b) – Normal mode elution SdFFF of the 0.2-0.8 μm fraction of Rocky Flats soils coupled with ICP-MS. (a) Fractogram representation of time versus mass Si and UV from FFF. (b) Converted fractogram into relative amount Si and UV versus diameter.

Representation of Fe and Al in the colloidal particles can be seen in Figure 3.7a, which is plotted with the UV response from the SdFFF. While Al has greater mass throughout the run, Fe is more symmetrical with the UV. This demonstrates that the Fe is more consistently representative throughout the particles in this size range. Both Fe and Al have similar void volume elution masses (20.5 and 23 percent of the mass, respectively) even though Al has more mass in the void peak. Figure 3.7b illustrates the lack of Fe coatings in colloids. There is, however, evidence of a possible mineralogy change. The smaller sized particles have an even ratio of Al and Fe, whereas the Al/Si ratio decreases in larger sized particles, while the Fe/Si ratio increases. This indicates that some sort of mineralogy change is occurring. The rise in Fe is most likely a mineralogical effect occurring, where the colloidal particles are transitioning from a kaolinite clay⁷ to perhaps an illite or vermiculite⁸. This can be further witnessed in the K/Si and Mg/Si ratios (Figure 3.7c). Both of the ratios have an identical shape to them, indicating that composition of the colloids at the larger sizes is increasing in Mg and K in relation to decreasing Si and Al, which is also consistent with the Fe. Figure 3.7d compares the size distributions of the Fe and Al with the UV. Both the Al and the Fe are similar in shape with the UV, which suggests they are dispersed within the colloidal particles. The Fe and Al in the particles represent 10.1 and 13.7 percent of the mass analyzed, respectively, making them secondary components of the colloids.

For the 0.2-0.8 micron size fraction, Mn and U were analyzed for the mass-based distributions, the results of which are represented in Figure 3.8a. Both of the trace elements seem to have higher concentrations in larger particle sizes, represented with broader peaks than the UV. The Mn peaks at approximately 21 minutes, whereas the U is approximately 16 minutes, which is closer to the UV peak elution time of 12 minutes. The Mn, as seen in the figure, has a high percentage of its mass in the void peak (approximately 26 percent), where the U has a more moderate amount (approximately

⁷ A kaolinite clay is mainly composed of Al, Si, and O.

⁸ Illites and vermiculites are soil that are highly composed of K, Mg, and Fe.

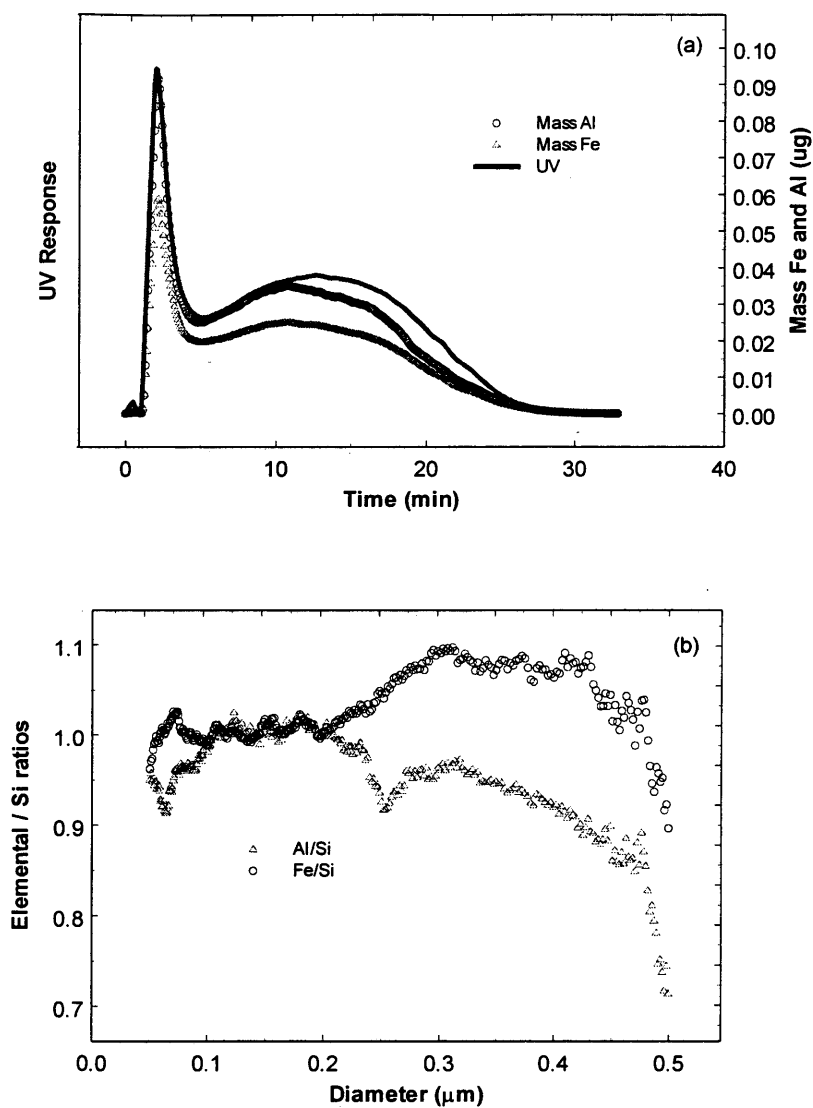


Figure 3.7 (a,b) - Normal mode elution SdFFF of the 0.2-0.8 μm fraction of Rocky Flats soils coupled with ICP-MS. (a) Fractogram representation of time versus mass Fe, Al, and UV from FFF. (b) Size representation of the Fe/Si and Al/Si ratios illustrating potential mineralogical changes in the colloids.

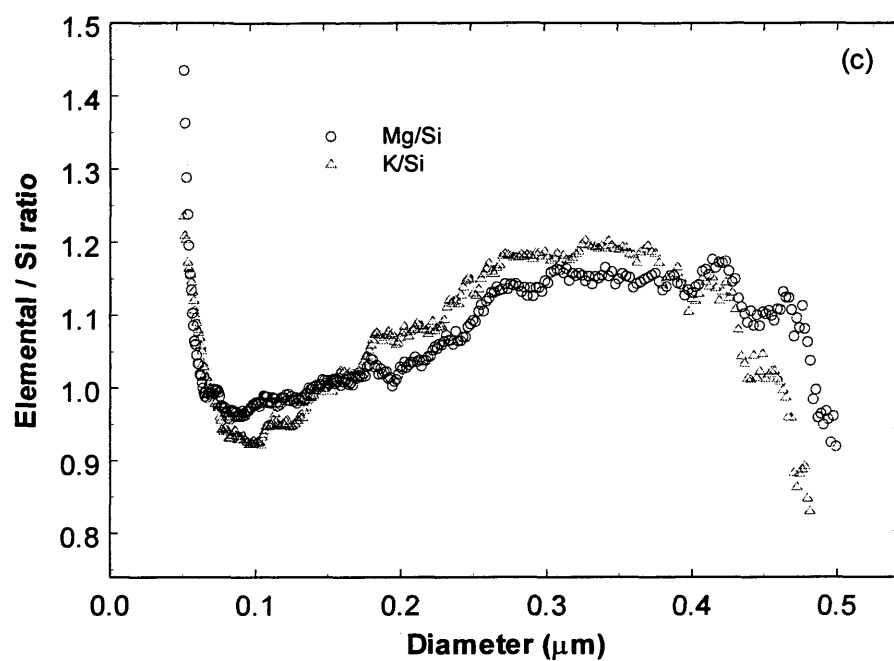


Figure 3.7c - Normal mode elution SdFFF of the 0.2-0.8 μm fraction of Rocky Flats soils coupled with ICP-MS. Representative of probable mineralogical changes and coatings present for the K/Si and Mg/Si ratios versus diameter.

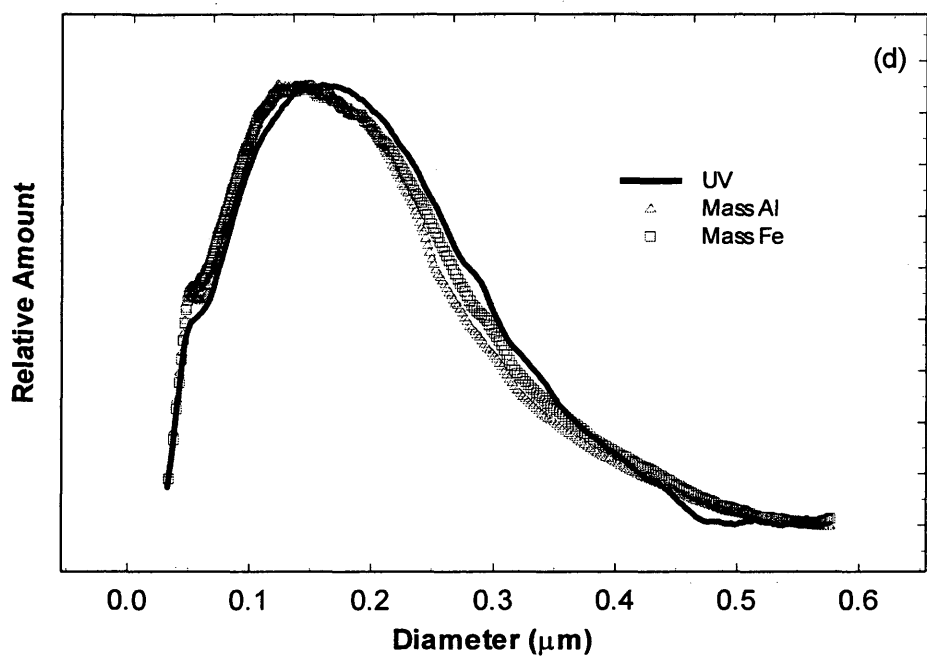


Figure 3.7d - Normal mode elution SdFFF of the 0.2-0.8 μm fraction of Rocky Flats soils coupled with ICP-MS. Converted fractogram into relative amount of Al, Fe, and UV versus diameter.

14.8 percent). This is indicative of more Mn mass in the dissolved phase, or in particles that were too small to be analyzed with the size analysis technique. Figure 3.8b illustrates the Mn/Si ratio, where it is important to notice that there is potentially a small amount of surface coatings on the particles. The more interesting result appears in the larger sizes, where a very significant increase of five times suggests a discrete manganese oxide phase in the larger particles. This is further proof of a mineralogical change occurring in the larger particles. The figure also yields a gradual change in the U/Si ratio. Overall, the U is dispersed throughout the colloid particles. Analysis of the relative amounts of Mn and U shown in Figure 3.8c illustrates the size distributions for the trace elements. The U has a lower relative amount in the smaller particles when compared with the UV, but larger particles seem to have similar relative amounts relative to the smaller sizes. The Mn is unusual because of its peak well after the UV has peaked, which means that the particles have a different composition at larger sizes. The U and Mn represent 0.00024 and 0.073 percent of the mass in the colloidal particles, respectively.

3.4 Conclusion

In order to understand the potential of natural soil colloids to transport sorbed contaminants through a porous media, it is important to understand the chemistry of the particles. Coupling a chemical composition analyzer such as ICP-MS with a size separation technique such as SdFFF shows the change of elemental compositions over a calculated size range. The technique is, however, subject to the limitations of the individual instruments, such as detection limits of chemical analysis techniques and shape effects on particle sizing.

Analysis of the soil samples yields a high concentration of Si, which is expected for natural soil colloids. Table 3.2 details the elemental percent mass of the two smallest size

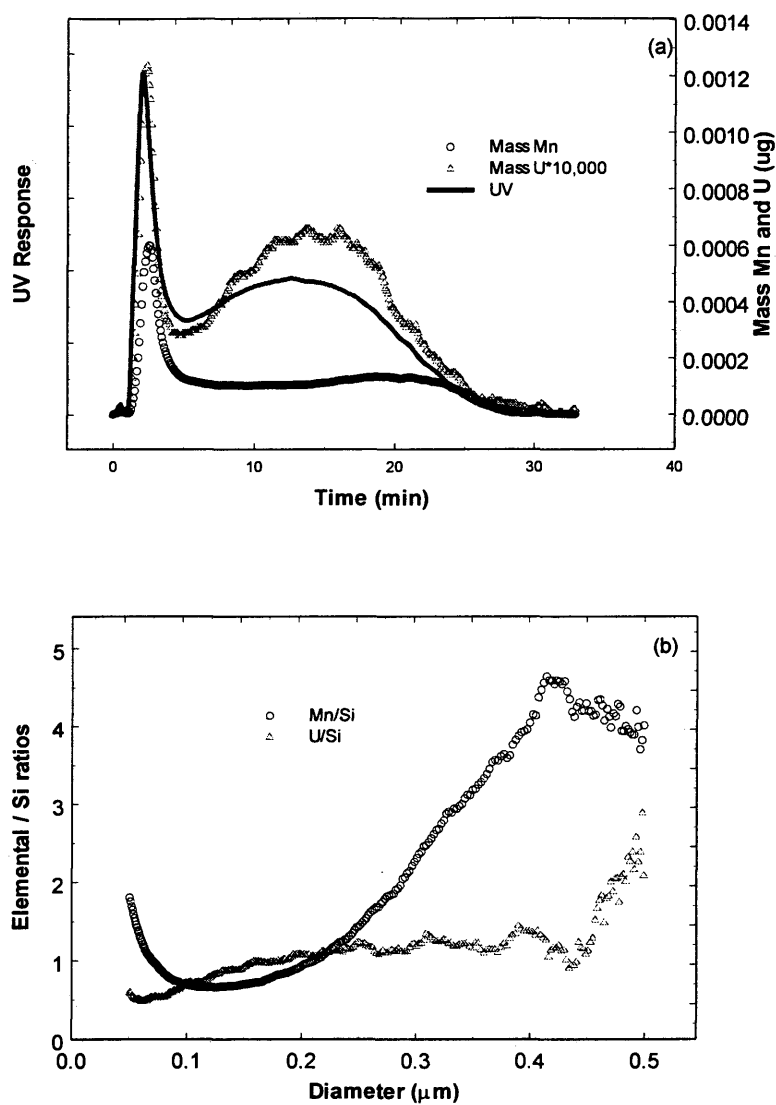


Figure 3.8(a,b) - Normal mode elution SdFFF of the 0.2-0.8 μm fraction of Rocky Flats soils coupled with ICP-MS. (a) Fractogram representation of time versus mass Mn, U, and UV from FFF. (b) Size representation of the Mn/Si and U/Si ratios.

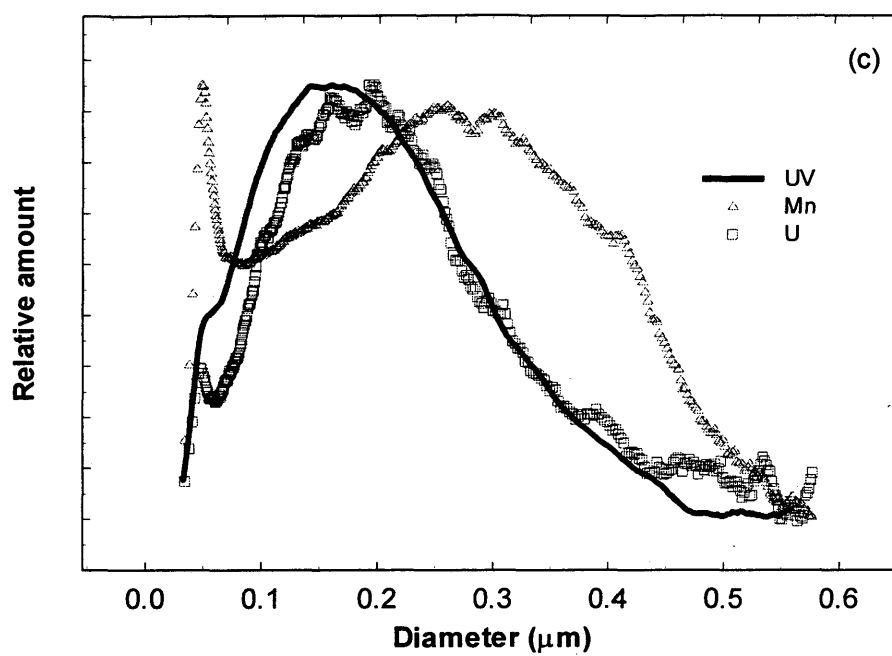


Figure 3.8c - Normal mode elution SdFFF of the 0.2-0.8 μm fraction of Rocky Flats soils coupled with ICP-MS. Converted fractogram into relative amount of Mn, U, and UV versus diameter.

fractionated samples. The percentages represent the total mass of an element eluted from the channel divided by the total mass of all the elements measured that were eluted from the channel. The analysis was able to successfully yield amounts of primary, secondary, and trace elements. These calculations are only representative of the elements measured. The soils could potentially be comprised of other elements, most likely in trace amounts. The table demonstrates that there is a significant difference in the elemental composition of the soils. Trace elements such as Mn and U did not change drastically between the two sizes. There was, however, an increase in the Fe, while a decrease in the Al. The other elements all decrease as a result of the dramatic increase in the percent mass of Si in the 0.2-0.8 micron fraction.

Table 3.2 - Percentage of elemental mass in Rocky Flats soils obtained by integration of the SdFFF-ICP-MS results.

Elemental Percentages								
Sample	Mg	Al	Si	K	Ca	Fe	Mn	U
<0.2 μm sample	3.2	22.0	54.5	4.0	4.8	8.3	0.08	0.00012
0.2-0.8 μm sample	1.80	13.70	69.30	1.30	1.50	10.10	0.07	0.00024

The mass eluted from the channel can be calculated for the elements analyzed, but it is not able to determine the mass retained in the channel, and if this retained mass has a molar ratio different from the injected or eluted mass. Bulk concentrations must be established to understand the retention in the channel. In order to determine changes in retention of molar ratios, a sample from each of the smaller two fractions was injected into the ICP-MS and analyzed. Table 3.3(a, b) shows the molar ratios of the elements sampled after elution from FFF compared with the initial concentrations in the centrifuged fractions (shown on the table as standard). The table presents the primary

Table 3.3(a,b) - Comparison of elemental ratios of bulk fraction and FFF run elution from channel using (a) Al and (b) Si to compare the elements.

(a) Elemental / Al ratios

Sample	Mg	Al	Si	K	Ca	Fe	Mn	U
<0.2 μm standard	0.189	1	2.077	0.184	0.283	0.261	0.004	1.67E-06
<0.2 μm FFF run	0.161	1	2.347	0.126	0.137	0.182	0.002	6.09E-07
FFF run / standard %	85.6	100.0	113.0	68.8	48.6	69.7	45.9	36.4
0.2-0.8 μm standard	0.146	1	1.937	0.121	0.039	0.268	0.004	2.89E-06
0.2-0.8 μm FFF run	0.145	1	4.788	0.067	0.066	0.355	0.0026	1.96E-06
FFF run / standard %	98.7	100.0	247.3	55.3	168.6	132.4	68.8	67.9

(b) Elemental / Si ratios

Sample	Mg	Al	Si	K	Ca	Fe	Mn	U
<0.2 μm standard	0.091	0.481	1.000	0.089	0.136	0.125	0.002	8.05E-07
<0.2 μm FFF run	0.069	0.426	1.000	0.054	0.059	0.077	0.001	2.59E-07
FFF run / standard %	75.7	88.5	100.0	60.9	43.1	61.7	40.7	32.2
0.2-0.8 μm standard	0.076	0.516	1.000	0.062	0.020	0.139	0.002	1.49E-06
0.2-0.8 μm FFF run	0.030	0.209	1.000	0.014	0.014	0.074	0.001	4.10E-07
FFF run / standard %	39.9	40.4	100.0	22.4	68.2	53.5	27.8	27.5

(Si), secondary (Mg, K, Ca, Al, and Fe), and trace elements (Mn and U). If the fractions were to have the same representation of the elements in the FFF results as the whole fraction, the FFF run divided by the standard percent value would be 100 percent. Table 3.3a represents the elemental/Al ratio. Most of the elements are less than or close to 100 percent with respect to Al for the size fractions ratio compared to the standard. Al has approximately five times more mass than the other secondary components. It also has almost exactly half the mass of Si in an injected sample. The Si potentially has been the least retained by the channel and therefore had the highest percentage of its material elute out of the channel. Table 3.3b shows that all the particles are less than 100 percent with respect to the Si, the trace elements are dramatically smaller. Overall, there was some retention of the particles in the channel in the course of the FFF run. Whether these particles have been retained because of their specific chemical composition is a potential research topic in the future.

CHAPTER 4

SUMMARY AND CONCLUSIONS

4.1 Summary of Results

Natural soil colloids play an important role in many processes that occur in the sub-surface environment. Most recently, they have been invoked to explain the subsurface transport of contaminants.

The research was organized into two main components: 1) particle size analysis and 2) chemical analysis versus size. In addition, a substantial amount of method development was undertaken in order to complete the established goals.

Centrifugation has traditionally been the method to separate particles in the 0.01-10 micron size range and is still used to obtain size fractions of the soil for analysis by other techniques. Centrifugation is limited by the same problems inflicted upon every other size analysis technique. Density difference among particles of the same size can produce substantially different results for methods such as SdFFF and centrifugation, which rely upon the sedimentation of particles to obtain size information. Other problems arise from shape effects, which are produced when non-spherical particles are able to give the appearance of being larger or smaller than they really are. This can affect techniques such as SEM, SPOS, PCS, centrifugation, and FIFFF.

The results from the analysis of each of these techniques yielded varying results depending on whether the method was number or volume based. SEM and SPOS are very similar when analyzing the results of their volume distributions of the two larger size fractions. Analyzing the volume distribution of smaller size fractions with SEM was not effective because a few number of larger particles skewed the results to large sizes. FFF yielded interesting results as well; FFF clearly favored the smaller sized particles in

the size distributions. Both of the FFF techniques, however, yielded similar results for the two smallest size fractions. The PCS results were inconclusive and not beneficial for analysis. It is not clear which of these methods actually is the most accurate, but every method resulted in the conclusion that there was a large majority of smaller particles in each of the soil fractions. From the results of the size analysis techniques, we are able to determine that centrifugation is difficult to have complete separation into well-defined fractions. Larger fractions will always have large numbers of smaller particles.

While it is a royal pain in the neck¹, FFF is a technique useful to a wide variety of applications: such as separation of viruses, the separation of polymers, and identification of natural soil colloids. Unlike most particle sizing techniques, FFF allows fractions to be collected and it can be coupled directly with chemical analyzers to give elemental comparisons with size. The SdFFF coupled to ICP-MS has been shown to be effective in the analysis of natural soil colloids for the determination of concentration of major, minor, and trace elements. Using the coupled system, it is possible to tell at what size particles change mineralogy and perhaps also determine where and how they were formed, whether they form from weathering, chemical or biological production, or are some form of biological debris. The change in elemental ratios can also be applied to surface coatings, which were found in small quantities on the Rocky Flats soil colloids, especially Mn and Fe. Overall, there is potential to study natural colloids in much greater detail using the coupled techniques.

4.2 Recommendations for Future Research

The results of this study have led to a number of questions, which will require more experimental work and expansion upon the methods that were developed for this research project.

¹ The instrument will most likely leave you as frustrated at times as it did for me.

1. Further research is needed to compare size analysis techniques. Each analytical instrument results in a different size distribution of the particles present.
2. A further comparison of online coupling of both the FIFFF and SdFFF to ICP-MS is warranted. Not only can the size distribution obtained by the two methods be compared, but also the amount of material retained in the channel with the different techniques can be compared.
3. In natural soil colloids, the particles are rarely (if ever) exactly spherical in shape. These particles can appear larger or smaller than they really are, which can make it hard to measure accurately. Is the retention time changed due to shape effect?
4. The importance of understanding colloidal transport is in the implication of this for potential transport of non-aqueous contaminant species. These could be anything from radionuclides to heavy metals or organics. Column experiments using natural soil colloids with a contaminant sorbed onto the surface of the particle could be conducted to see the effects of the contaminant on retention, particle size, etc. In the case of metals on radionuclides, coupling an FFF technique with ICP-MS could determine which size contained the most contaminant and which had the greatest potential for transport.

REFERENCES CITED

- Buffle, J. and G.G. Leppard. Characterization of aquatic colloids and macromolecules. 1. structure and behavior of colloidal material. *Environ. Sci. Technol.* (1995), Vol. 29, No. 9: 2169-2175
- Buffle, J. and G.G. Leppard. Characterization of aquatic colloids and macromolecules. 2. key role of physical structures on analytical results. *Environ. Sci. Technol.* (1995), Vol. 29, No. 9: 2176-2184
- Butcher, David J. and Joseph Sneddon. A Practical Guide to Graphite Furnace Atomic Absorption Spectrometry. New York: John Wiley and Sons, Inc., 1998.
- Chittleborough, David J., Deirdre M. Hotchin, and Ronald Beckett. Sedimentation field-flow fractionation: a technique for the fractionation of soil colloids. *Soil Science* (1992), Vol. 153, No. 5: 341-348.
- Contado, Catia, Gabriella Blo, Francesco Fagioli, Francesco Dondi, and Ronald Beckett. Characterization of River Po particles by sedimentation field-flow fractionation coupled to GFAAS and ICP-MS. *Colloids and Surfaces A: Physicochemical and Engineering Aspects* (1997), 120: 47-59.
- Deguelldre, Claude, Ines Triay, Jae-Il Kim, Peter Vilks, Marcus Laaksoharju, and Norbert Miekeley. Groundwater colloid properties: a global approach. *Applied Geochemistry* (2000), 15: 1043-1051.
- Elimelech, Menachem, Masahiko Nagai, Chun-Han Ko, and Joseph N. Ryan. Relative insignificance of mineral grain zeta potential to colloid transport in geochemically heterogeneous porous media. *Environ. Sci. Technol.* (2000) 34: 2143-2148.
- Hassellöv, Martin, Benny Lyvén, Conny Haraldsson, and Waraporn Sirinawin. Determination of continuous size and trace element distribution of colloidal material in natural water by on-line coupling of flow field-flow fractionation with ICPMS. *Anal. Chem.* (1999), Vol. 71, No. 16: 3497-3502.
- Kaplan, Daniel I., Paul M. Bertch, Domy C. Adriano, and William P. Miller. Soil-borne mobile colloids as influenced by water flow and organic carbon. *Environ. Sci. Technol.* (1993), 27: 1193-1200.

- Martin, Michel and P. Stephen Williams. Theoretical basis of field-flow fractionation. Theoretical Advancement in Chromatography and Related Separation Techniques. Boston, MA: Kluwer Academic Publishers, 1992.
- McCarthy, John F. and John M. Zachara. Subsurface transport of contaminants: mobile colloids in the subsurface environment may alter the transport of contaminants. *Environ. Sci. and Technol.* (1989), Vol. 23, No. 5: 496-502.
- Ranville, James R., David J. Chittleborough, Finlay Shanks, Richard J.S. Morrison, Thomas Harris, Faber Doss, and Ronald Beckett. Development of sedimentation field-flow fractionation-inductively coupled plasma mass-spectrometry for the characterization of environmental colloids. *Analytica Chimica Acta* (1999), 381:315-329.
- Ranville, James R. and Ronald L. Schmiermund. Chapter 2. An Overview of Environmental Colloids. Perspectives in Environmental Chemistry. D.L. Macalady, ed. New York: Oxford University Press, 1998.
- Ryan, Joseph N. and Philip M. Gschwend. Effects of ionic strength and flow rate on colloid release: relating kinetics to intersurface potential energy. *Journal of Colloid and Interface Science* (1994), 164: 21-34.
- Schimpf, Martin, Karin Caldwell, and J. Calvin Giddings, ed. Field-Flow Fractionation Handbook. New York: John Wiley and Sons, Inc., 2000.
- Seaman, John C. Thin-foil SEM analysis of soil and groundwater colloids: reducing instrument and operator bias. *Environ. Sci. Technol.* (2000), 34: 187-191.
- Skoog, D.A. and Leary, J.J. Principles of Instrumental Analysis, Fourth Edition. Orlando, FL: Harcourt Brace College Publishers, 1992.
- Tadjiki, Soheyl. Studies on the Characterisation and Behaviour of Soil Colloids Using Field-Flow Fractionation. PhD Dissertation, Monash University, 1999.
- Welz, Bernhard and Michael Sperling. Atomic Absorption Spectrometry, 3rd ed. New York: Wiley-VCH, 1999.
- Williams, P. Stephen, Myeong Hee Moon, and J. Calvin Giddings. Influence of accumulation wall and carrier solution composition on lift force in

sedimentation/steric field-flow fractionation. *Colloids and Surfaces* (1996) 113:215-228.

Yao, K.M., T. Habibian, and C.R. O'Melia. Water and waste water filtration, concepts and applications. *Environ. Sci. Technol.* (1971), 5: 1105.